Impact of Temperature and SO_4^{2-} on Electrostatic Controls over Carbonate Wettability

Joel T. Tetteh[1*], Patrick V. Brady[2] and Reza Barati Ghahfarokhi[1]

[1] Department of Chemical and Petroleum Engineering, University of Kansas

[2] Sandia National Laboratories, USA

[*]Correspondence to: Joel T. Tetteh (E-mail: joel_tetteh@ku.edu)

Key Highlights

- A surface complexation model was developed which describes high temperature calcite-brine-oil interfaces.
- Increasing temperature decreased oil-calcite electrostatic bonding and increased water wetness in calcite rocks.
- Increasing temperature enhanced brine imbibition into limestone, as predicted by the surface complexation model.
- Sulfate concentration and brine pH also influenced calcite wettability.

Abstract

The use of modified salinity and modified composition brines (MSMC), referred to as smart water, to alter carbonate surface wettability at different temperatures has gained enormous popularity. However, an effective way to quantify the geochemical, thermodynamic and electrostatic factors responsible for wettability alteration have still not been fully developed. In this work, a surface complexation model (SCM) based on geochemical and thermodynamic interactions at calcite and oil surfaces was used to investigate the effect of temperature, pH, and sulfate on electrostatic interactions. SCM's for calcite and oil surfaces were validated against zeta potential data at high temperatures and used to interpret improved oil recovery data from spontaneous imbibition experiments. The SCM was correlated to calcite wettability through the calculation of the bond product sum (BPS); a measure of the strength of the electrostatic bond linkages between calcite and oil surfaces. Increasing temperature increased the zeta potential towards more positive for positive polarities and more negative for negative polarity at both the calcite and oil surfaces. BPS decreased with increasing temperature due to the weakening of [$>CO_3^-$][$-NH^+$] electrostatic bonds, indicating an increase in water-wetness, consistent with the existing literature. Increasing the sulfate ion concentration in seawater brine reduced the BPS, indicating an increase in water wetness. This was attributed to the reduction in [$>CaOH_2^+$][$-COO^-$] associated bonds as sulfate concentration increased. Spontaneous imbibition experiments confirmed the BPS analysis, whereby oil recovery increased as sulfate concentration and temperature increased.

1 Introduction

Low salinity waterflooding has been investigated intensely in recent years mainly due to the cost effectiveness of the technique. In sandstone formations, low salinity waterflooding usually involves reducing brine ionic strength to improve recovery [1]. In carbonates however, improved recovery can require both brine ionic strength reduction and modified the concentrations of specific ions, i.e. "smart" waterflooding [2–8].

The positive response of low salinity and smart waterflooding in carbonate formations has been documented using techniques such as coreflooding, contact angle, zeta potential and spontaneous imbibition [4,9–11]. Nasralla et al. [10] observed improved oil recovery of ~ 7.5% in tertiary mode using seawater brine and 25 times diluted seawater from a reservoir limestone from the Middle East. Austad and coworkers [12–14] have extensively developed the concept of potential determining ions (PDIs) influencing wettability alteration process in carbonates. They proposed a multivalent ionic exchange process involving the PDIs (i.e. Mg^{2+}, Ca^{2+}, and SO_4^{2-}) to be responsible for wettability alteration leading to improved oil recovery from

chalk formations. Zhang, et al., [14] highlighted the effect of calcium and sulfate as wettability modifiers whereby an increase in calcium concentration resulted in improved recovery at 100-130°C. Zhang, et al., observed that, above 130°C, magnesium becomes more important than calcium in wettability alteration [12]. Austad et al., showed that for wettability alteration to be triggered in limestone using low salinity brine, the limestone must contain anhydrite, which would dissolve and release SO_4^{2-} which in turn altered wettability [15]. Tetteh et al [8] showed through statistical analysis of improved oil recovery data from different carbonate rocks that SO_4^{2-} was not directly correlated with improved oil recovery, but temperature was correlated with improved recovery. Sohal et al [16] in a similar statistical analysis observed that Mg^{2+} rather than SO_4^{2-} was better correlated with observed improved oil recovery from carbonates. Song et al.[17] showed through imbibition and surface complexation modeling that sulfate caused wettability alteration and improved oil recovery from Indiana limestone at 90°C. The imbibition data was interpreted with a surface complexation model developed for 25°C conditions. Mahani et al [18] showed through disjoining pressure calculations that, the stability of the water film was dependent on the temperature of the brine solution. Lu et al [19], observed a decrease in water contact angle (WCA) with an increase in temperature. However, zeta potential measured at the calcite-brine interface remained relatively the same after increasing temperature from 25°C to 50°C. Strand et al [20] indicated that increasing temperature during low salinity waterflooding could trigger better improved oil recovery. However, the improved oil recovery was attributed to dissolution of anhydrite. Thus, the effect of SO_4^{2-} and temperature on crude oil-brine-rock systems remains unclear.

Zeta potential measurements are typically used to link interfacial chemistry to rock wettability [18,21–27] as they can quantify the role of disjoining pressure at the crude oil-brine-rock (COBR) interface [28]. Zeta potential tracks the thinning or thickening of the water film separating the rock and crude oil macromolecules affecting the three point contact line and hence rock wettability [29–31]. The same zeta potential polarity at the rock and oil interfaces would result in repulsive disjoining pressure causing thickening of the water film, hence a water-wet rock. Opposite polarity would result in attractive disjoining pressure, thinning of the water film and oil-wetness [7,28,30]. Whereas most coreflooding and contact angle measurements are performed at high temperatures, zeta potentials are usually measured at laboratory temperature, ~25°C due to equipment limitations. Sari et al., performed zeta potential measurements at 25°C to interpret contact angle data and improved oil recovery data from corefloods both at 60°C [32]. Zhang et al. measured zeta potentials of chalks at 25°C to explain wettability alteration observed in spontaneous imbibition experiments performed at ~ 90°C [14]; other wettability and zeta potential measurements performed at different temperatures include references [30,33]. However, Mahani et al measured contact

angles up to 100ºC and zeta potential at temperatures as high as 70ºC, on carbonate rocks [18]. Increasing temperature apparently resulted in no significant wettability shift in limestones and a slight wettability shift in dolomites [18]. Lu et al also measured water contact angle and zeta potential at 25ºC and 65ºC on a calcite surface using NaCl and $MgCl_2$ solutions at different concentrations [34]. They observed a decrease in the water contact angle as temperature increased whiles zeta potential remained relatively the same at the different temperatures. But in theory, temperature should influence wettability and zeta potential because the Debye length, which affects the thickness of the double layer and hence influences the surface potential, is a function of temperature. The dielectric constant, which affects the charge distribution on a surface, is also a function of temperature. Thus, the total disjoining pressure at the COBR interface is influenced by temperature.

The traditional use of electrophoresis to measure zeta potential is limited by salinity and temperature [35]. Most electrophoresis devices have a temperature ceiling of 60ºC; stable colloids cannot be maintained at high temperature and the electrodes degrade rapidly in high salinity brines[35]. Streaming potential technique has been used determine rock zeta potentials at high salinities and high temperatures. Collini et al., used streaming potential technique to measure zeta potential on intact reservoir core (100% brine saturated) at temperatures as high as 100ºC [35]. Ayirala et al., also used streaming potential to measure zeta potential from 25ºC to 60ºC and observed that the magnitude of the zeta potential increased with temperature [36]. However, streaming potential setups are not common in petroleum engineering related research labs, and require a long time to acquire experimental data. As a result, calcite zeta potential data at high temperature are difficult to come by.

In the absence of high temperature zeta potential measurements, SCM's which describe the molecular and chemical interactions between a particle and aqueous solution could be used to predict zeta potential, and explore rock wettability, at high temperature [37–47]. Brady et al developed an SCM to predict the electrostatic behavior of sandstone surfaces at high temperatures by using reaction enthalpies derived from the literature [48]. Xie et al.[49] and Mansi et al.[50] both used the SCM developed by Brady et al. [48] to investigate the effect of temperature on sandstone, observing a low salinity response at elevated temperature. However, the SCM should be more extensively validated at higher temperature.

SCM's have only infrequently been used to investigate carbonate electrostatic interaction at higher temperature. Brady and Thyne [42], used an SCM with estimated enthalpy values to predict improved oil recovery using the bond product sum from a coreflood performed on carbonate rock by Yousef et al [4] at 100ºC. Sanaei et al. [51] predicted oil recovery data at 120ºC measured by Chandresekhar et al. [52] using UTCOMP-IPhreeqc by implementing an SCM. However, in both cases, the SCM was not validated against

zeta potential data. The objective of this work was to provide a mechanistic understanding of the effect of SO_4^{2-} and temperature on electrostatic adsorption influencing carbonate wettability. Here, we test the ability of an experimentally validated SCM to predict calcite zeta potentials at elevated temperature and examine the ability of seawater-like brines with excess sulfate to release more oil from limestones. The SCM developed by Brady et al., [42] and modified by Tetteh et al., [21,22] was used for the investigation. The SCM was used to explain the effect of pH and sulfate on rock and oil surface charge. Spontaneous imbibition experiments using the seawater-like brines were done on Indiana limestone rock at different temperatures to quantify the effect of temperature on rock wettability and improved recovery. This work provides novelty in detailing mechanistic thermodynamic process associated with electrostatic controls on calcite surface wettability due to the combined effect of temperature, pH and sulfate concentration as fully examined using a SCM, backed with wettability alteration data and improved oil recovery experiments. This work begins by detailing the material used for zeta potential and spontaneous imbibition experiments. A detailed SCM, procedure for spontaneous and zeta potential measurements was described in the method section. The results section discussed the impact of temperature, SO_4^{2-} and pH on the electrostatic controls at the COBR interface. The observations in this work were compared to published data in the discussion section to further elucidate on the factors influencing carbonate wettability interface. This work showed that the desired wettability state of a carbonate surface could be attained by influencing the electrostatic bonds through the use of brine solution with sufficient SO_4^{2-} ions and temperatures above 50C.

2 Material and Methodology

2.1 Rock

Indiana limestone (purchased from Kocurek Industries) was used in spontaneous imbibition experiments and zeta potential analysis[21,22]. The rock cores were cut to an average length of about 3 inches (7.6 cm) and average diameter of 1.5 inches (3.8 cm), allowed to dry in an 80-90ºC oven, and saturated with formation water salinity (FWS) brine to serve as the connate water. The rock porosity and pore volume were calculated by measuring the dry and wet weight before and after the brine saturation, respectively, and the measured bulk volume. The rock permeability was measured by force flooding the 100% water saturated core with FWS brine at three different flowrates (1ml/min, 2ml/min and 3ml/min) for about three pore volumes for each. The Darcy equation was the applied to calculate the rock permeability. Initial water saturation was established by force flooding the 100% water saturated core with LKC crude oil for ~5 pore volumes and until pressure drop across the core has stabilized. Cores were subsequently aged statically in a 90ºC oven for a period of 40 days to establish oil-wetness. XRD analyses of cores indicated >99% calcite

[53]. Core properties are listed in **Table 1**.

Table 1: Indiana Limestone properties

Core	Pore Volume	Porosity	Permeability (mD)	S_{oil}	Length, cm	Diameter, cm
IL_1	15.87	19.07	105.39	0.72	7.46	3.77
IL-2	16.03	19.40	68.09	0.75	7.45	3.76
IL-3	15.85	18.83	248.32	0.77	7.56	3.77
IL-4	14.74	17.68	53.49	0.80	7.52	3.76
IL-5	14.13	17.22	40.98	0.81	7.37	3.77
IL-6	14.71	17.20	80.00	0.61	7.40	3.83
IL-7	14.82	17.60	119.00	0.51	7.51	3.78

2.2 Brine

Synthetic FWS brine had a composition similar to that from the Lansing Kansas City (LKC) limestone group of the Trembley ranch field in Kansas. The initial seawater composition (SWS) was five-times diluted FWS [21,22,54,55]. The sulfate concentration was low in the SWS brine (52 ppm) and was therefore increased 25 and 50 times to form SWS25*S and SWS50*S respectively by sodium sulfate addition. **Table 2** shows the chemical composition of the brines used. The synthetic brines were prepared by adding different amounts of NaCl, KCl, $MgCl_2.6H_2O$, $CaCl_2.2H_2O$ and Na_2SO_4, purchased from Fisher Scientific except for $MgCl_2.6H_2O$, to deionized water. $MgCl_2.6H_2O$ was purchased from Sigma Aldrich for the brine preparation. All chemicals used for the brine preparation were ACS grade.

Table 2: Composition of brine solution used for the SCM calculations.

Ions, ppm	FWS, ppm	SWS, ppm	SWS25*S	SWS50*S
Ca^{2+}	11,000	2,200	2,200	2,200
Mg^{2+}	2,800	560	560	560
Na^{+}	48,000	9,600	9,640	9,640
K^{+}	500	100	100	100
Cl^{-}	101,913	20,382	19,523	18,564
SO_4^{2-}	260	52	1,300	2,600
Brine pH	5.12	5.57	5.59	5.50
IS, mol/L	3.27	0.65	0.67	0.68
TDS, ppm	164,473	32,895	33,323	33,664

2.3 Crude Oil

Reservoir oil samples from the limestone members of the LKC group were used for the experiment. Unfiltered crude oil was used to preserve the heavier oil components which can affect brine-oil interactions being studied. LKC crude oil had a viscosity and density of 5.86 cp and 0.84 g/cm^3 at 40^{o}C, respectively.

Total acid and base numbers were 0.17 mg KOH/g and 0.11 mg KOH/g, respectively; asphaltenes content was 0.73 wt%.

2.4 Surface Complexation Model

PHREEQC simulator (version 3.4), an open source geochemical solver from the USGS widely used to model groundwater chemistry, was relied on for the SCM simulations [56]. Calcite surfaces are modeled to be made up of two hydration sites which protonate or deprotonate to form positively and negatively charged surface species [21,25,57,58]. Reactions at the calcite surface were modelled using >CaOH and $>CO_3H$ as the primary hydration sites [37,42,43]. The hydration sites for the oil surface were -NH and -COOH, the amine base and carboxylic acid components, respectively. These come from the measured total base and acid numbers, TBN and TAN respectively (see below).

The surface charge (σ_{DL}) of the oil and calcite surfaces was calculated by summing the product of the species concentration (m_s) and charge of the surface complexes (v_{si}) based on protonation and deprotonation reactions between the colloidal surfaces and the aqueous species (**Equation 1**).

$$\sigma_{DL} = \frac{F}{AS}\sum m_s v_{si} \qquad \textit{Equation 1}$$

where A is the specific surface area (m^2/g) of the particle; S is the solid concentration (g/L); and m_s is the concentration of surface species (mol/m^2) [37]. Surface species concentrations were calculated from mass action equations based on a series of presumed surface reactions and their equilibrium constants (**Table 3**). The diffuse double layer model was used to compute the surface potential (ψ) from the calculated surface charge, using the Gouy-Chapman equation [59]:

$$\sigma_{DL} = 0.1174 I^{0.5} \sinh\left(\frac{F\psi}{2RT}\right) \qquad \textit{Equation 2}$$

where I is the ionic strength of the solution, *F* is Faraday's constant, R is the universal gas constant and T is absolute temperature.

The zeta potential was estimated based on the simplification of the Poisson-Boltzmann equation (for zeta potential $\leq \pm 25$ mV), generating the Debye-Hückel equation [59,60] below

$$\zeta = \psi \exp(-\kappa d_s) \qquad \textit{Equation 3}$$

where ζ is the zeta potential at the slipping plane, d_s is the distance between the Stern layer and the slipping plane, and κ is the inverse of the Debye length, which is expressed as:

$$\kappa^{-1} = \sqrt{\frac{\varepsilon_r \varepsilon_o k_b T}{2 N_A e^2 I}} \qquad \textit{Equation 4}$$

where ε_r is relative permittivity of solution; ε_o is the permittivity, 8.854E-12 $F.m^{-1}$ [61]; k_b is Boltzmann

constant, 1.381E-23 $J.K^{-1}$; e is the charge of an electron, N_A is Avogadro's number, T is temperature, and *I* is the ionic strength of the solution. The product of κ and d_s was set at 0.33 nm based on published slipping plane and ionic strength relationships [57,62].

The reactions used for the surface species concentration and their sorption equilibrium constants (K) are listed in **Table 3** for both calcite and oil surfaces. For example, the intrinsic K value for reaction 1 was calculated as:

$$K = \frac{[>CaOH_2^+]\exp(F\psi/RT)}{[>CaOH]\{H^+\}} \qquad \textit{Equation 5}$$

where bracket [..] denote concentration (mol/m^2) and bracket {..} denote thermodynamic activities [42]. The intrinsic K values (**Table 3**) were modified using the relation below for the apparent K value considering the system temperature

$$K_{app} = K_{int} * exp\left(\frac{-zF\psi}{RT}\right) \qquad \textit{Equation 6}$$

where K_{int} and K_{app} are the intrinsic and apparent K values, respectively at 25°C. The temperature dependence of K values were defined using the Van't Hoff equation [59]:

$$\frac{d\ In\ K}{dT} = \frac{\Delta H_r}{RT^2} \qquad \textit{Equation 7}$$

where ΔH_r is the reaction enthalpy. The reaction enthalpy was assumed to be constant over the range of temperatures considered. Equation 7 was used to solve for K values at different temperatures. The reaction enthalpies for the oil surface reactions were taken from Erzuah et al.,[38] while the rock surface reaction enthalpies were calculated based on log K values at 25°C and 120°C presented by Sanaei et al[63].

Table 3: Input parameters for the SCM.

Surface		Reaction	logK at 25°C	Enthalpy (kJ/mol)
Calcite	1	$>CaOH + H^+ \leftrightarrow >CaOH_2^+$	11.85	-50.0
	2	$>CaOH_2^+ + SO_4^{2-} \leftrightarrow >CaSO_4^- + H_2O$	2.1	-9.4
	3	$>CaOH + HCO_3^- \leftrightarrow >CaCO_3^- + H_2O$	5.8	-30.7
	4	$>CO_3H \leftrightarrow >CO_3^- + H^+$	-5.1	-14.1
	5	$>CO_3H + Ca^{2+} \leftrightarrow >CO_3Ca^+ + H^+$	-4.4	2.3
	6	$>CO_3H + Mg^{2+} \leftrightarrow >CO_3Mg^+ + H^+$	-4.4	-4.4
Oil	7	$-NH^+ \leftrightarrow -N + H^+$	-5.5	34.0
	8	$-COOH \leftrightarrow -COO^- + H^+$	-4.6	0.0

	9	-COOH + Ca^{2+} ↔ -$COOCa^{+}$ + H^{+}	-3.6	1.2
	10	-COOH + Mg^{2+} ↔ -$COOMg^{+}$ + H^{+}	-3.4	1.2

The –COOH and –NH hydration site densities were calculated from the TAN and the TBN, respectively, using Equation 8 [38]:

$$\text{Oil site density (site/nm}^2) = \frac{\text{TAN or TBN}}{M_W \text{ of KOH (g/mol)}} * \frac{N_A}{\text{A}} \qquad \textit{Equation 8}$$

where M_w is the molecular weight of potassium hydroxide (KOH), which is 56.105 g/mol. The –COOH and -NH site densities were calculated to be 1.825 site/nm^2 and 1.18 sites/nm^2 respectively using the specific surface area of oil as 1 m^2/g [38]. A calcite specific surface area of 1 m^2/g [64] and site density of 4.95 sites/nm^2 [65] were used to define the calcite surface. These parameters provided a good fit to zeta potential values measured for different brine composition in our previous experimental data and data from the literature [21,22], supporting the validity of the SCM.

Temperature and pH were varied from 25ºC to 150ºC and 5 to 8, respectively, representing most carbonate reservoir conditions. pH was varied by adding HCl or NaOH. The Debye length was calculated for each brine system and used to define the electrical double layer (EDL) thickness in the diffuse double layer model. PHREEQC was used to maintain equilibrium with calcite, i.e. to account for calcite dissolution that might occur during the zeta potential measurement. For all the SCMs, the system was equilibrated with atmospheric CO_2 at $P_{CO2} = 10^{-3.4}$ atm.

Zeta potentials were predicted, then surface species concentrations were calculated for both the oil and rock surfaces. From calculated oil and calcite surface speciation, the association of the positively charged species at the calcite surface with negatively charged species at the oil surface and vice-versa were summed (**Equation 9**, the BPS [38,42]) to quantify electrostatic interaction between oil and calcite [21,22,42,43]. **Figure 1** illustrates electrostatic potential bond linkages between calcite and oil surfaces.

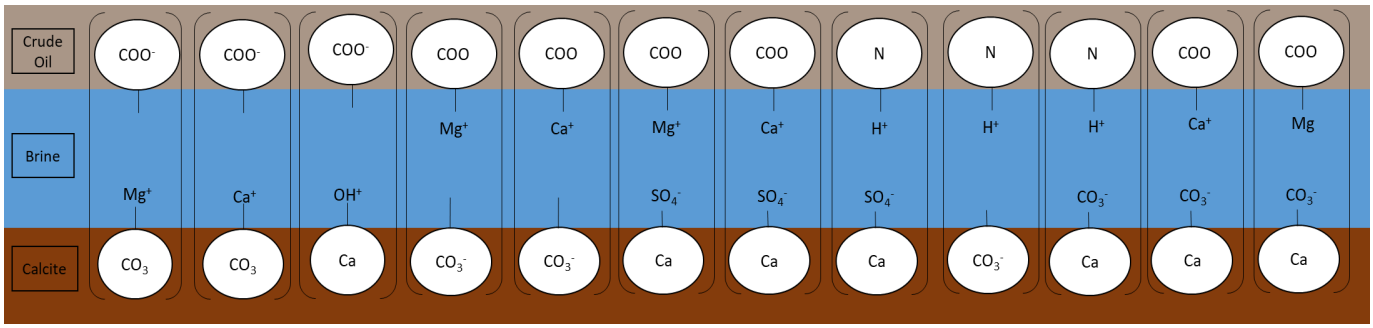

Figure 1: Electrostatic bond interaction at the COBR interface influencing the rock wettability [21,62]**.**

$$BPS=[NH^+][CaSO_4^-]+[NH^+][CaCO_3^-]+[COO^-][CO_3Mg^+]+[COO^-][CO_3Ca^+]$$
$$+[COOCa^+][CO_3^-]+[COOCa^+][CaSO_4^-]+[COOCa^+][CaCO_3^-]+$$
$$[COOMg^+][CO_3^-]+[COOMg^+][CaSO_4^-]+[COOMg^+][CaCO_3^-]+$$
$$[NH^+][CO_3^-]+[COO^-][CaOH_2^+] \qquad \textit{Equation 9}$$

2.5 Spontaneous Imbibition Tests

After FWS core saturation and aging, core samples were placed in imbibition cells and immersed in the appropriate brine solution at different temperatures to evaluate changes in rock wettability caused by sulfate concentration and temperature. **Table 4** shows the experimental sequence used for the imbibition experiments. The cell was completely sealed to avoid any loss of fluid from the cell. Due to density differences between the brine and crude oil, the produced oil goes on top of the water in the graduated section. The volume was recorded until no oil was produced for at least four days continuously.

Table 4: Summary of experimental sequence used for the imbibition experiments

Ex	Core ID	Sequence of imbibition			Purpose
1	IL-1	SWS at 30°C	SWS at 50°C	SWS at 70°C	Impact of temperature and sulfate concentration on wettability changes
2	IL-2	SWS25*S at 30°C	SWS25*S at 50°C	SWS25*S at 75C	
3	IL-3	SWS50*S at 30°C	SWS50*S at 50°C	SWS50*S at 70°C	
4	IL-4	SWS at 30°C	SWS25*S at 50°C	SWS25*S at 70°C	Impact of temperature and sulfate concentration on wettability changes and IOR in tertiary mode
5	IL-5	SWS at 30°C	SWS50*S at 50°C	SWS50*S at 70°C	

A full set of imbibition experiment (brine and oil imbibition) was also used to calculate the Amott-Harvey wettability index (**Equation 10** [66]) for both FWS and SWS, after aging and after seawater-like brine imbibition (spontaneous and forced imbibition measurements were performed at 40°C to replicate reservoir conditions).

$$I_{A-H} = I_w - I_o \qquad \textit{Equation 10}$$

I_{A-H} is the Amott- Harvey index, I_w is the Amott water index, calculated as:

$$I_w = \frac{V_{os}}{V_{os}+V_{of}} \qquad \textit{Equation 11}$$

where V_{os} is the total volume of oil produced after spontaneous water imbibition and V_{of} is the total oil produced after forced water imbibition through coreflooding.

I_o is the Amott oil index and calculated as:

$$I_o = \frac{V_{ws}}{V_{ws}+V_{wf}} \qquad \textit{Equation 12}$$

where V_{ws} is the total volume of water produced after spontaneous oil imbibition and V_{wf} is the total water produced after forced oil imbibition through coreflooding. Amott-Harvey indices fall into one of three categories: $-1 \leq I_{wo} \leq -0.3$ is an oil-wet system, $-0.3 < I_{wo} < 0.3$ is intermediate- or mixed-wet and $0.3 \leq I_{wo} \leq 1$ is water-wet ([67].

Table 5 shows the water and oil Amott index, and the Amott-Harvey wettability index measured for the aged Indiana limestones. The use of SWS brine as imbibing brine, after rock aging using FWS brine shifted rock wettability from oil-wet to mixed wet (**Table 5**). Note that I_{A-H} accounts for capillary pressure shifts caused by rock wetting changes. Capillary pressure can be related to the total disjoining pressure by assuming that the pressure in the thin film separating the oil and rock is identical to the pressure within the wetting fluid [8,30]. The total disjoining pressure is also influenced by electrostatic forces. Therefore, spontaneous imbibition, which is a component of the I_{A-H}, can be used to interpret the electrostatic controls to wettability alteration. The static water contact angle on limestone measured in FWS brine was 157°, hence oil-wet, consistent with the I_{A-H} observation. Again, SWS brine decreased the contact angle to 115°, indicating a shift to intermediate wetness (See [21] for the contact angle data). Thus, additional improved oil recovery observed beyond that for SWS brine would indicate more wettability alteration towards water wetness.

Table 5:Amott and Amott-Harvey wettability indices for aged Indiana limestone cores and their corresponding wettability state.

Brine	Cores	I_w	I_o	I_{A-H}	Wettability State
FWS	IL-6	0.19	0.46	-0.26	Oil-wet
SWS	IL-7	0.60	0.49	0.12	Mixed-wet

3 Results and Discussion

3.1 Model validation

The SCM for calcite and oil surfaces were validated by Tetteh et al., [21,22] for 25°C and 40°C against measured zeta potentials from single salt brines of ionic strength of 0.04M, formation water, seawater and low salinity brines at 25°C and 40°C [21]. The SCM matched data trends from measured zeta potentials and as a function of temperature. The SCM also matched rock zeta potential data from Alotaibi and Yousef

[68] and Ding and Rahman [64] and oil zeta potential data of Alshakhs and Kovscek [30]. Tetteh et al. [22] further validated the SCM by fitting zeta potential trends of calcite and oil measured in different seawater and low salinity brines at 25°C and 40°C.

Calcite zeta potentials in seawater brines measured as a function of temperature are shown in the supporting information (SI, **Figure A1**). Zeta potential measurements followed the procedure established in our previous publications. An average of four (4) measurements each with three (3) runs was presented as the zeta potential. Standard deviation was within ±3mV of each system. The SCM predicted the temperature-dependent measured zeta potential trends. In general, an increase in temperature resulted in an increase in the measured and predicted zeta potential. SCM predicted the carbonate zeta potential up to 80°C from Collini et al [35] and Alotaibi and Yousef [68] (**Figure A1**) A site density of 0.5 site/nm^2 and a specific surface area of 1m^2/g was used in both calculations. Thus, SCM appears to predict the trends seen in the limited number of high temperature zeta potential measurements. Nevertheless, more experimental data at higher temperatures is needed to more precisely constrain the role of temperature on calcite electrostatics.

Due to the lack of experimental data and the experimental complexities associated with measuring oil-brine zeta potential at higher temperatures, the current SCM for oil-brine interface was only used to measure zeta potential at 25 and 40°C as presented in our previous publications [21,22]. While the streaming potential measurement in the oil aged limestone rock has been interpreted as oil-brine zeta potential, the presence of the rock sample would introduce additional electrostatic and geochemical interactions during the rock aging period, hence was not considered in our SCM predictions.

3.2 Effect of temperature and sulfate on the calcite surface at different pH's.

Figure 2 and 3 shows changes in surface species concentrations calculated by the validated SCM as a function of temperature and sulfate concentration from pH 5 to 8. Reservoir pH in carbonate formations usually ranges between 5 to 8 [8], and reservoir temperatures ranges from 40-50°C for carbonate formation in the central Kansas uplift [54,69] to as high 120°C for carbonate formations in the Middle East. As sulfate increased by fifty times from SWS (52ppm) to SWS50*S (2600ppm), the concentration of the >$CaSO_4^-$ species increased (**Figure 2**). This was accompanied by a decrease in concentration of the dominant species (both >$CaOH_2^+$ and >CO_3^-) at the calcite surface, making the surface more negative [30,68,70] with sulfate. This is similar to observations by Brady and Thyne [42] using brine compositions from Yousef et al., [4]. It should be noted that >CO_3- was more abundant than all positively charged species, especially >$CaOH_2^+$, at pH 8, which would make the calcite surface more negatively charged with increasing temperature. This observation is consistent with literature were by >$CaOH_2^+$ and >CO_3^- species were the largest contributors to calcite surface charge and hence would influence rock wettability the most[21,43–46,58]. At pH 5-7,

$>CaOH_2^+$ dominated calcite speciation, remaining relatively constant or slightly increasing as temperature increased due to high sorption constant used for reaction 1. However, at pH 8, reaction 1 shifts to left which results in the decrease in $>CaOH_2^+$ species at the surface. For example, the concentration of $>CaOH_2^+$ species for SWS brine decreased from 1.6 µmol/m^2 at pH 7 to 1.56 µmol/m^2 at pH 8, calculated at 25°C, consistent with literature [44,46,58,71]. Chen et al [44–46,58], observed that the concentration $>CaOH_2^+$ was constant at low pH but began to decrease at solution pH of 7-8 and above. The temperature trends of $>CaOH_2^+$ is related to the adsorption of SO_4^{2-} ion onto the calcite surface. The adsorption of sulfate ion on calcite increased with increasing temperature at low pH (pH of 5). At pH 7 and 8, $>CaSO_4^-$ decreased with increasing temperature. At pH 8, the reaction 2 shifts to the left as temperature increases due to negative reaction enthalpy, which caused the logK value to reduce. This resulted in reducing SO_4^{2-} adsorption onto the calcite surface, thereby increasing the concentration of the primary hydration site, i.e. >CaOH, which drives reaction 1. Reduction in $>CaOH_2^+$ and $>CO_3^-$ concentrations in response to sulfate adsorption would reduce the overall electrostatic attraction and ultimately alter rock wettability to more water wetness.

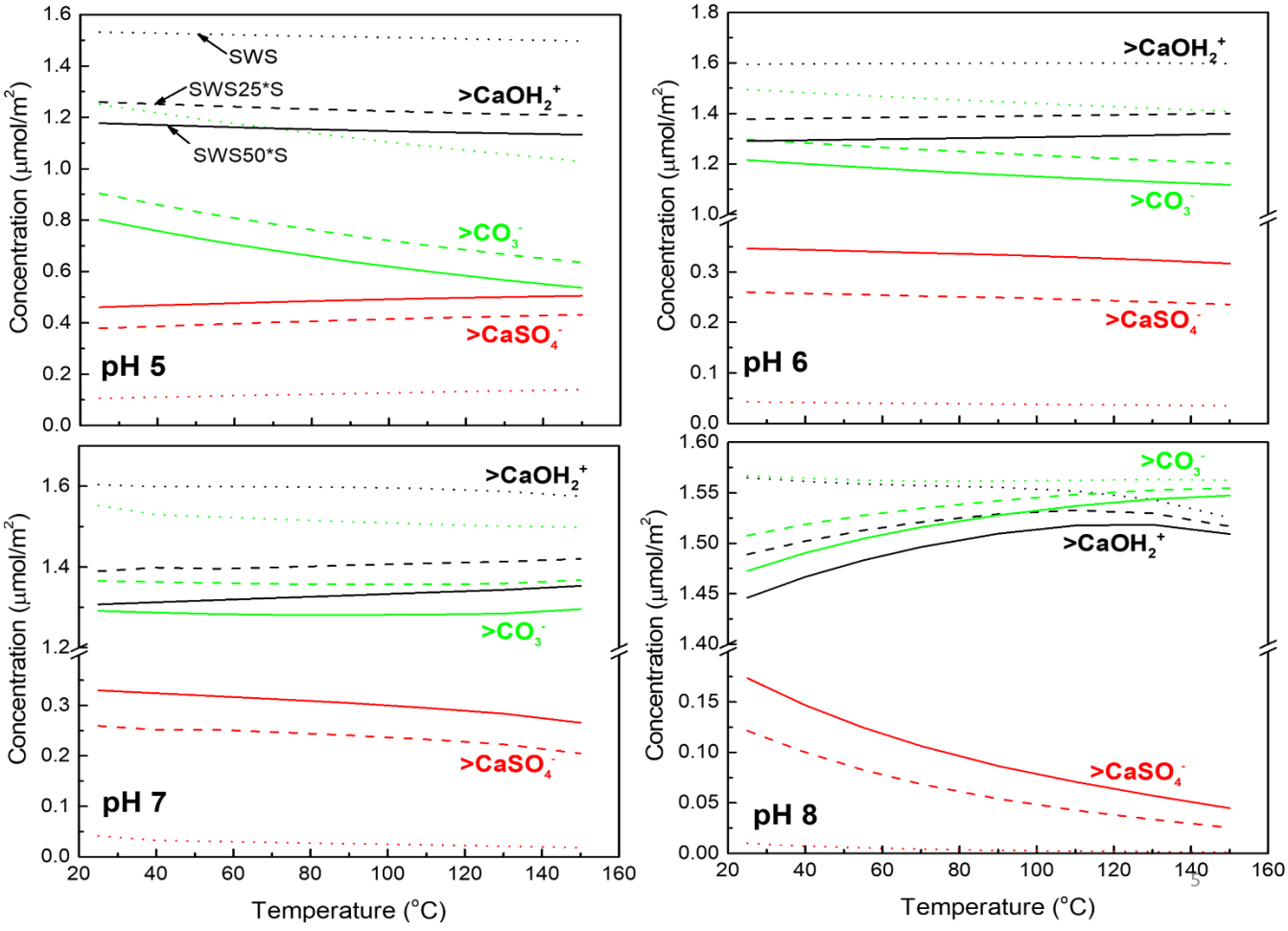

Figure 2: Variation in calculated $>CaSO_4^-$, $>CO_3^-$ and $>CaOH_2^+$ species as a function of temperature and pH. Dotted line is for SWS, dashed line for SWS25*S and solid lines for SWS50*S.

Both $>CO_3Ca^+$ and $>CO_3Mg^+$ decreased with increasing temperature at pH 5 and 6 (**Figure 3**). At pH 7 and 8, the adsorption of Ca^{2+} and Mg^{2+} with temperature varied. Increasing temperature resulted in increased adsorption of Ca^{2+} to calcite while Mg^{2+} adsorption decreased. Increasing sulfate adsorption to calcite is accompanied by increased adsorption of Ca^{2+} and Mg^{2+}, consistent with the wettability alteration mechanism proposed by Zhang et al [14,72].

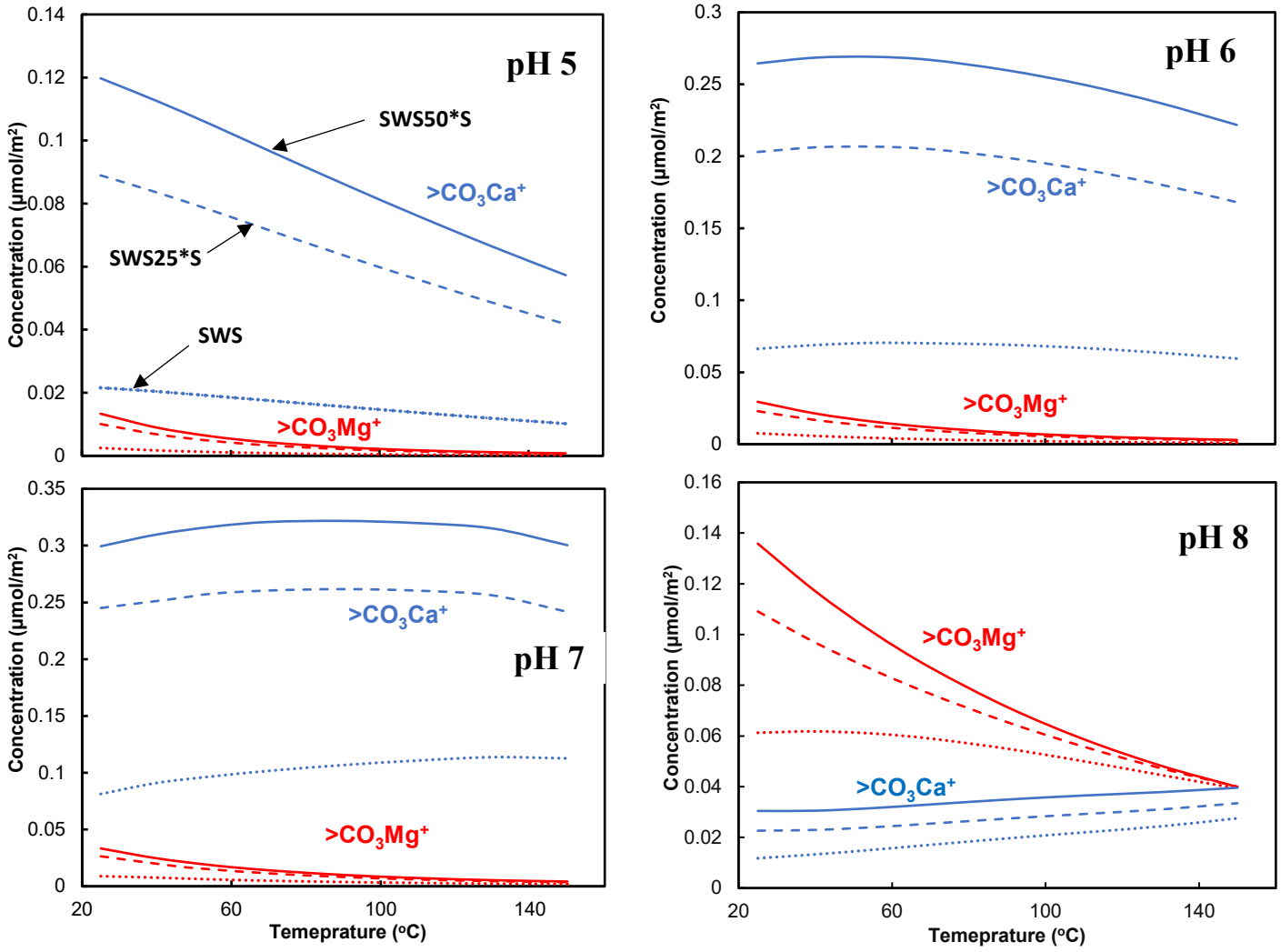

Figure 3: Variation in $>CO_3Ca^+$ and $>CO_3Mg^+$ concentration as a function of system temperature at different pH. Dotted line represents SWS, dashed line represents SWS25*S and solid lines represents SWS50*S

Zeta potential, which gives an indication of the stability of the water film influencing wettability was calculated as a function of pH and temperature for each brine system using the Debye-Hückel equation (**Equation 3**) - see **Figure 4**. In all cases, the calcite zeta potential decreased as pH increased. The zeta potential increased with increasing temperature from brine pH 5 to 7 due to the dominance of $>CaOH_2^+$. The concentration of $>CO_3^-$ at pH 8 increased with increasing temperature and increased the negative zeta potential. The highest zeta potential was calculated for SWS brines with the value decreasing as the sulfate

concentration increased due to the increased sulfate adsorption and reduced $>CaOH_2^+$. A negative calcite zeta potential can thus be caused by high brine pH (above pH 7) and high sulfate (SWS25*S and SWS50*S brines).

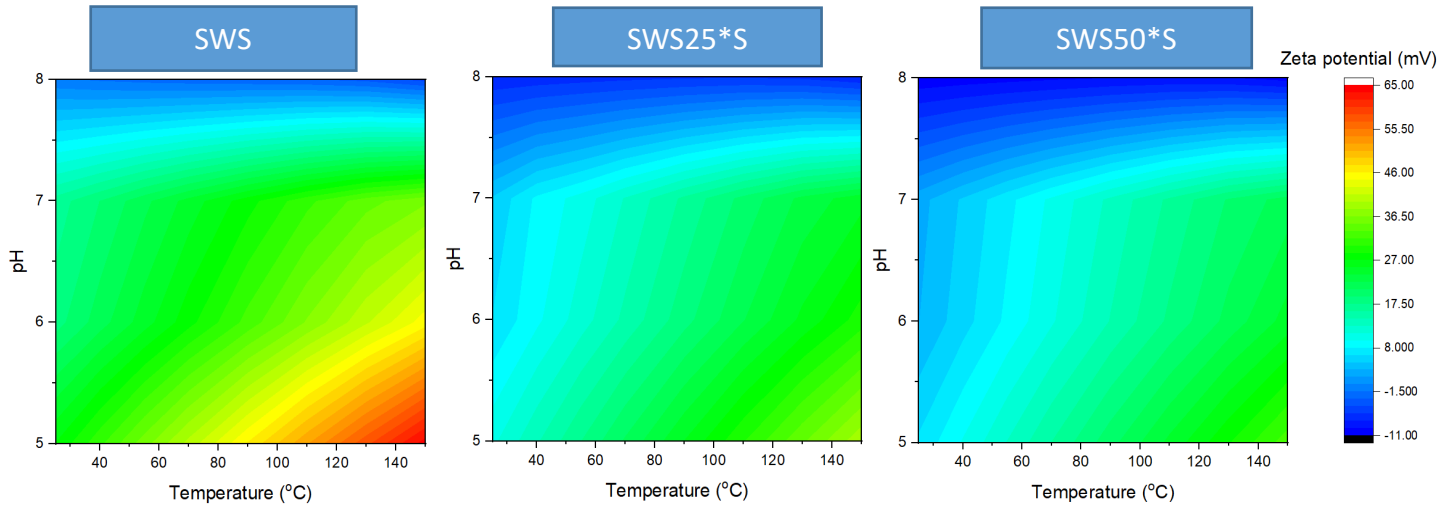

Figure 4: Variation in zeta potential at the calcite surface as a function of system temperature and pH for seawater-like brines. Reservoir pH usually varies between 5 to 8 in carbonate rocks.

3.3 Effect of temperature and sulfate on the oil surface at different pH's.

Figure 5 shows oil surface speciation as a function of temperature from pH 5 to 8. $-NH^+$ decreased sharply with temperature and pH for all the brines. For example, at pH 5, the $-NH^+$ concentration was calculated to be 0.29 µmol/m^2 at 25°C, but dropped to 0.05 µmol/m^2 at 150°C. $-NH^+$ concentrations fell to 0.0023 at pH 8 and 25°C, consistent with observations in the literature [21,43,46]. Decreased $-NH^+$ concentrations would decrease electrostatic interaction between the amine basic molecules of the crude oil and the negatively charged species ($>CO_3^-$, $>CaSO_4^-$ and $>CaCO_3^-$) on the calcite surface and make the system more water-wet. The effect of sulfate on the electrostatic linkers, $-NH^+$ and $-COO^-$ species, is minor. An increase in sulfate only slightly affects $-COOCa^+$ and $-COOMg^+$, which could be attributed to the slight difference in the brine salinities. Sulfate ion is not known to interact with the oil surface and is usually not included in the sorption reactions at the oil surface [42,48,73].

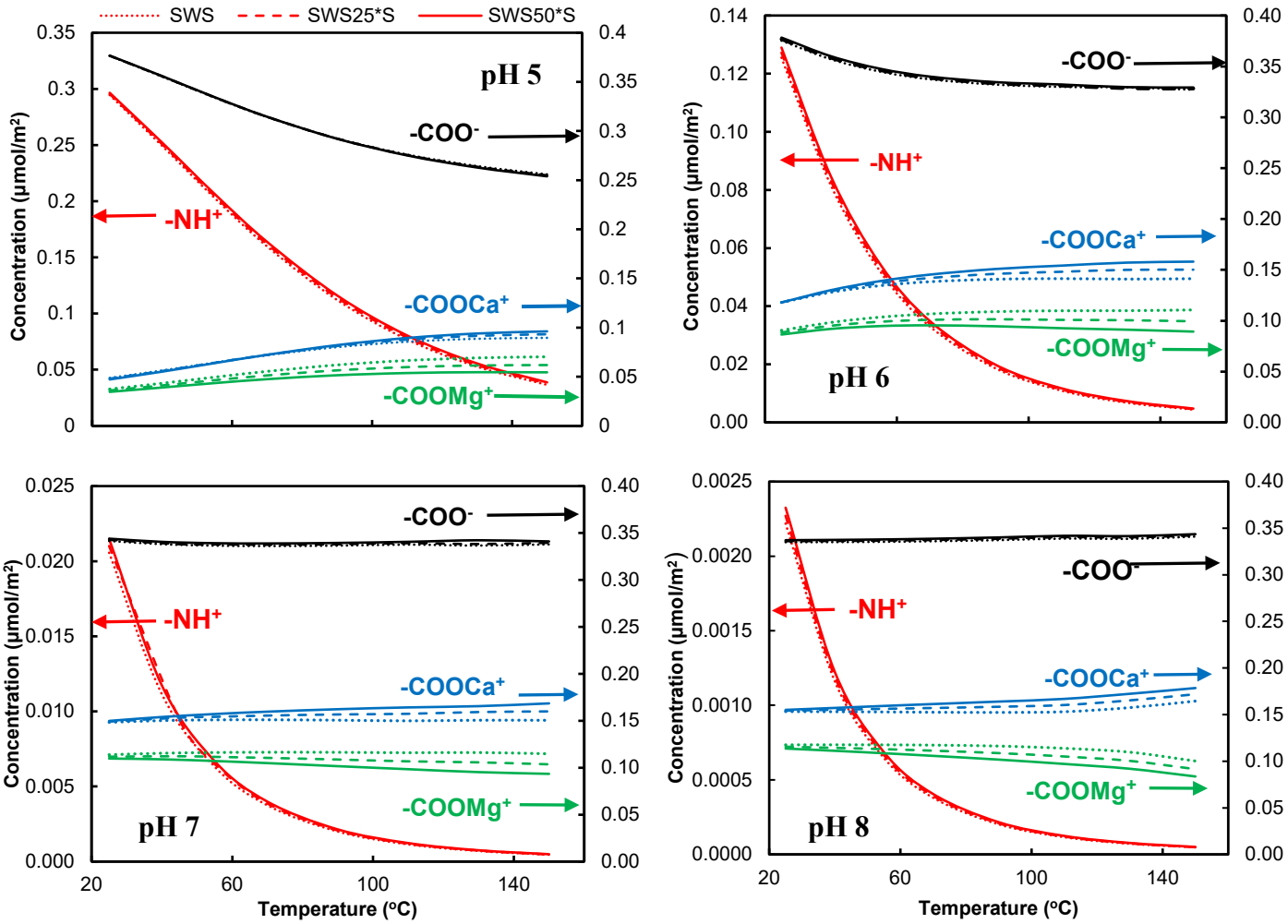

*Figure 5: Variation in surface species as a function of system temperature for oil surfaces at different pH. The arrows indicate the axis for each species. Dotted line represents SWS, dashed line represents SWS25*S and solid lines represents SWS50*S*

Calculated oil zeta potential decreases with temperature (**Figure 6**), primarily because of the sharp decrease in $-NH^+$. Whereas the concentrations of $-COO^-$ was similar at different pHs (e.g. about 3.7E-7 and 3.4E-7 mol/m^2 for pH 5 and 8 respectively at 25°C), that of $-NH^+$ varied greatly as pH increased, consistent with literature [21,45,50,74–76]. The concentration of the other positive species ($-COOCa^+$ and $-COOMg^+$) varies slightly with temperature and pH. Based on this observation, reservoir pH and temperature should cause a negative oil zeta potential hence, a negative zeta potential at the calcite surface would prompt a repulsive disjoining pressure and make calcite more water wet. It should be noted that **Figure 6** provides the extended trends in zeta potential measurement with respect to temperature and solution pH. However, in actual zeta potential measurements, uncertainties due to experimental procedure, materials and atmospheric conditions could affect the absolute value of the measured zeta potential.

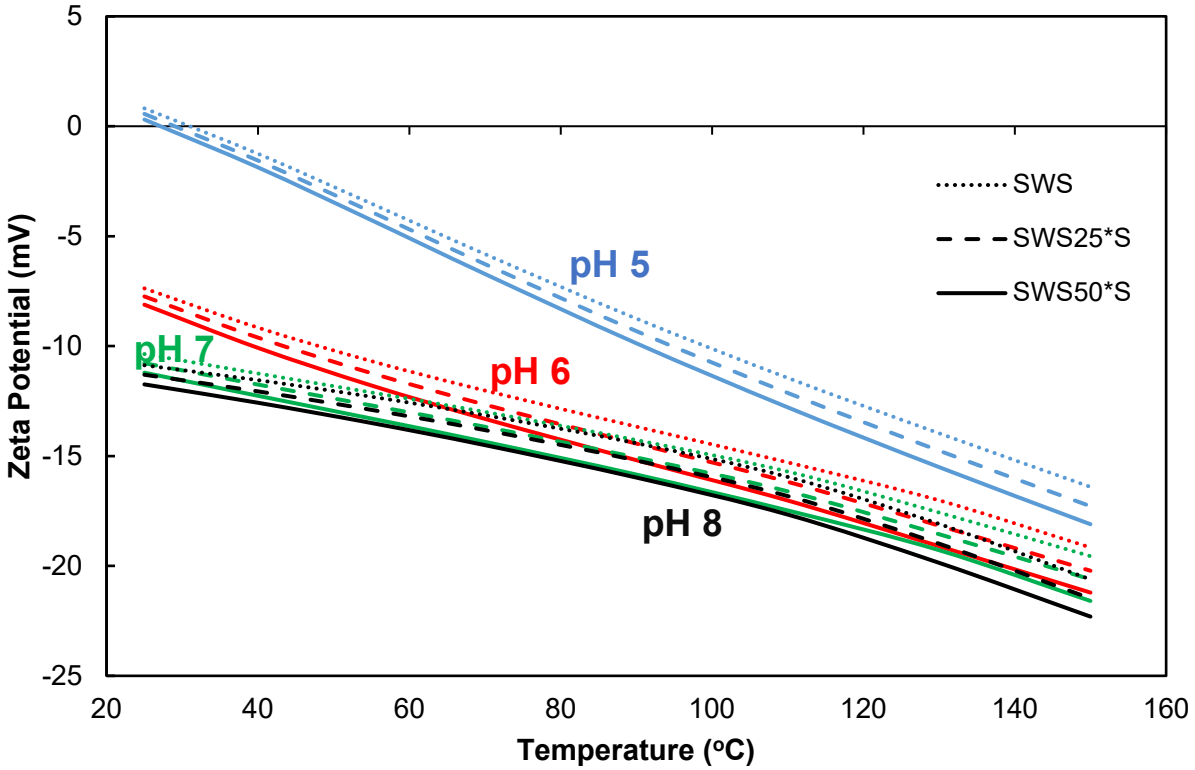

*Figure 6: Variation in zeta potential at the oil surfaces as a function of system temperature and pH for seawater-like brines. Dotted lines represent SWS, dashed lines represent SWS25*S and solid lines represent SWS50*S.*

3.4 Effect of temperature and sulfate on electrostatic controls

Figure 7 shows calculated concentrations of dominant electrostatic bonds as a function of temperature from pH 5 to 8. Other electrostatic bonds as a function of temperature were presented in SI (Figure A2). The dominant ones are [$>CaOH_2^+$][$-COO^-$] and [$>CO_3^-$][$-NH^+$] (**Figure 8**). Increasing temperature decreases [$>CaOH_2^+$][$-COO^-$], [$>CO_3^-$][$-NH^+$] and [$>CaSO_4^-$][$-NH^+$] at pH 5 to 8. But at pH 8, [$>CaOH_2^+$][$-COO^-$] decreases from 25°C to 110°C, after which it plateaus for SWS50*S and slightly decreases for the other brines (**Figure 7**). This observation could be attributed to the behavior of $>CaOH_2^+$ at pH 8, which was driven by the adsorption of SO_4^{2-} on calcite surface with increasing temperature at pH 8, and the reaction enthalpy for reaction 1. This observation was explained in section 3.2 and shown in **Figure 2**. At pH 8, the concentration of $-COO^-$ was observed to be relatively constant with increasing temperature and hence affected the temperature trends at pH 8 of [$>CaOH_2^+$][$-COO^-$] less. At all brine pH's the BPS decreases with temperature, predicting increased water-wetness and better oil recovery (**Figure 8**). At temperature above ~50°C, low pH favors water-wetness (**Figure 8**).

Elevated sulfate adsorption at the surface decreases the number of otherwise predominant bonds, [$>CaOH_2^+$][$-COO^-$] and [$>CO_3^-$][$-NH^+$] (**Figure 7**). In other words, the adsorption of sulfate prompts desorption of the carboxylic and amine links of the crude oil to the calcite surface, resulting in a more water-

wetness as observed with the BPS calculations (**Figure 8**). This is consistent with literature observations of sulfate altering rock wettability and improving oil recovery in carbonates [12,15,42,77,78]. The key point from **Figure 8** is that water wetness (low BPS) is favored at elevated temperature, high sulfate concentration, and low pH consistent with literature [17,18,21,23,42,58,64,73,79,80].

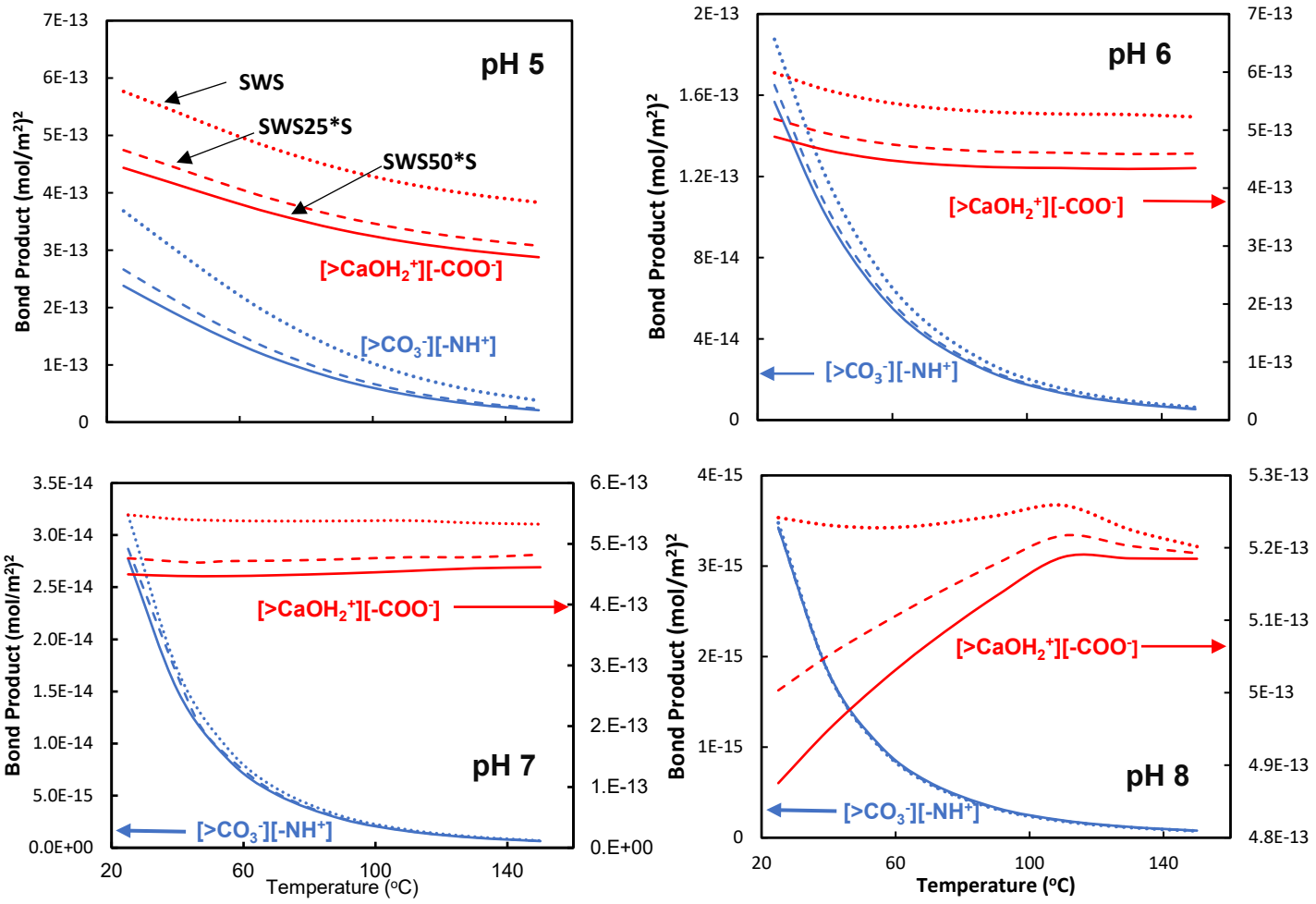

*Figure 7: Variation in [>CaOH₂⁺][-COO⁻] and [>CO₃⁻][-NH⁺] electrostatic bond linkages as a function of temperature at pH 5 to 8. Dotted lines represent SWS, dashed lines represent SWS25*S and solid lines represent SWS50*S.*

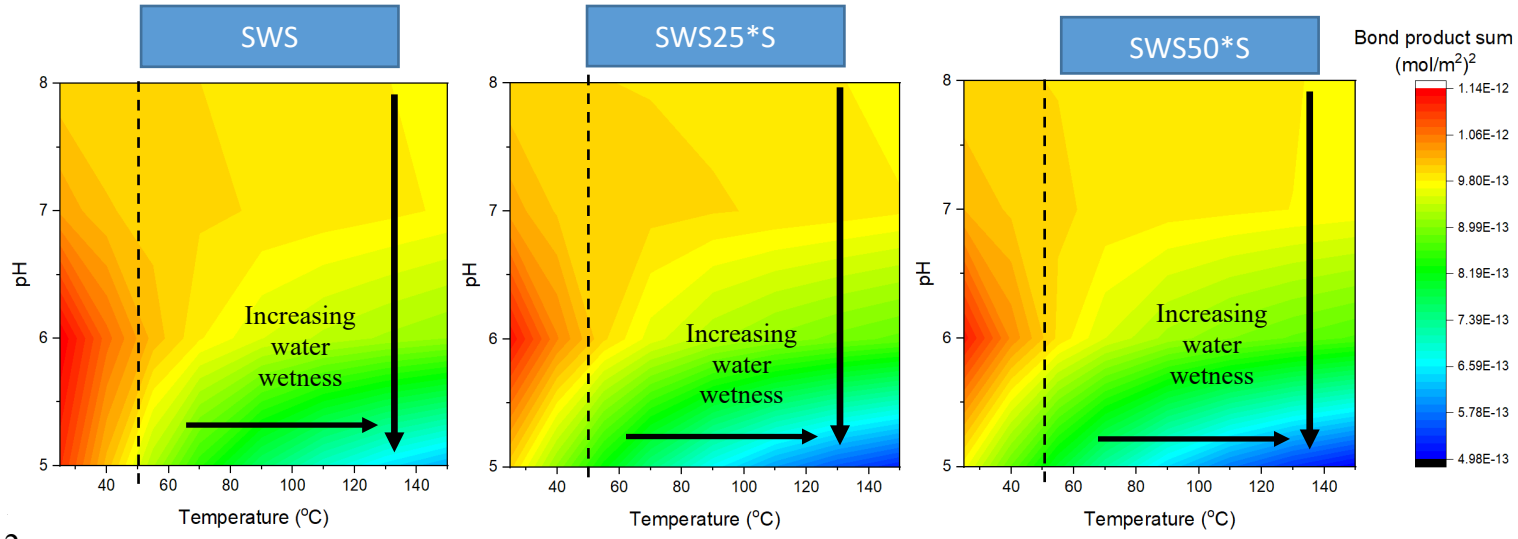

Figure 8: Variation in BPS as a function of system temperature and pH for seawater-like brines. Temperatures to the right of the dashed lines represent most carbonate reservoir temperatures. The direction of the arrows indicates the direction of increasing water wetness.

3.5 Effect of temperature and sulfate on wettability and improved oil recovery

Figure 9 shows oil recovery from spontaneous imbibition tests done in primary mode at 30°C on aged limestone using seawater-like brines with different sulfate concentrations. This experiment was performed to explore the effect of sulfate concentration on oil recovery and served as a baseline used to quantify the effect of temperature on oil recovery. Due to the long aging time and the low imbibition temperature, oil recoveries were low in primary mode similar to previous observations in the literature [17]. Song et al observed ~5% oil recovery from Indiana limestone core after aging the for 2 weeks in 120°C conditions. Nevertheless, an increase in sulfate concentration improved oil recovery, consistent with the BPS calculations.

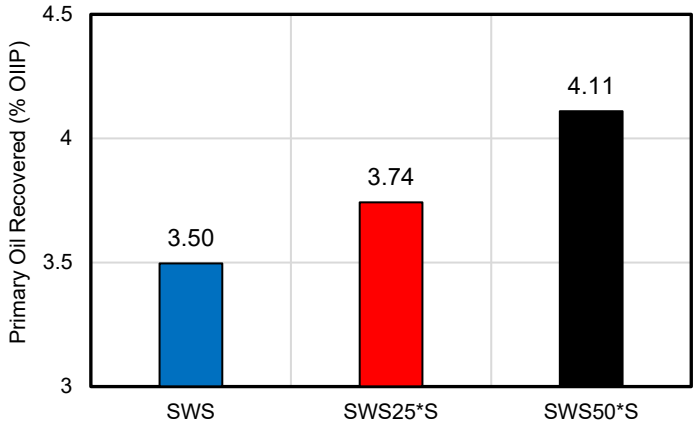

Figure 9: Oil recovered using spontaneous imbibition in primary mode at 30°C for different sulfate concentration in seawater-like brines.

The ability of higher temperatures and higher sulfate levels to improve oil recovery after primary imbibition is shown at 50°C and 70°C in **Figure 10**. The imbibition brine used in primary mode was the

same, but temperature was increased for both the secondary and tertiary modes. SWS25*S showed the sharpest increase in oil recovery, adding 12.06% and a further 9.15% more oil after switching temperatures to 50°C and finally to 70°C, respectively. SWS50*S brine also improved recovery better than the base SWS brine after switching temperatures, adding a total of 19.72% of the oil initially in place (OIIP) to the overall oil recovery. Similar trends have been observed in the literature [13,23,30,77,78,81,82]. Austad and coworker has observed that SO_4^{2-} and temperature are required to trigger the wettability alteration process in carbonate rock for improved oil recovery[12,13,83]. It should be noted that greatest improved oil recovery observed by SWS25*S could be indicative that an optimum sulfate concentration could trigger wettability alteration. Awolayo et al [84] also observed an optimum SO_4^{2-} concentration beyond which improved oil recovery was very marginal. Awolayo et al [84] attributed the observation to the possibility of anhydrite formation at such high SO_4^{2-} concentration, which could inhibit oil production in the cores and at the field scale. Nevertheless, it was observed in this work that, increasing sulfate concentration plays an impactful role in increasing the oil recovery in carbonate rocks.

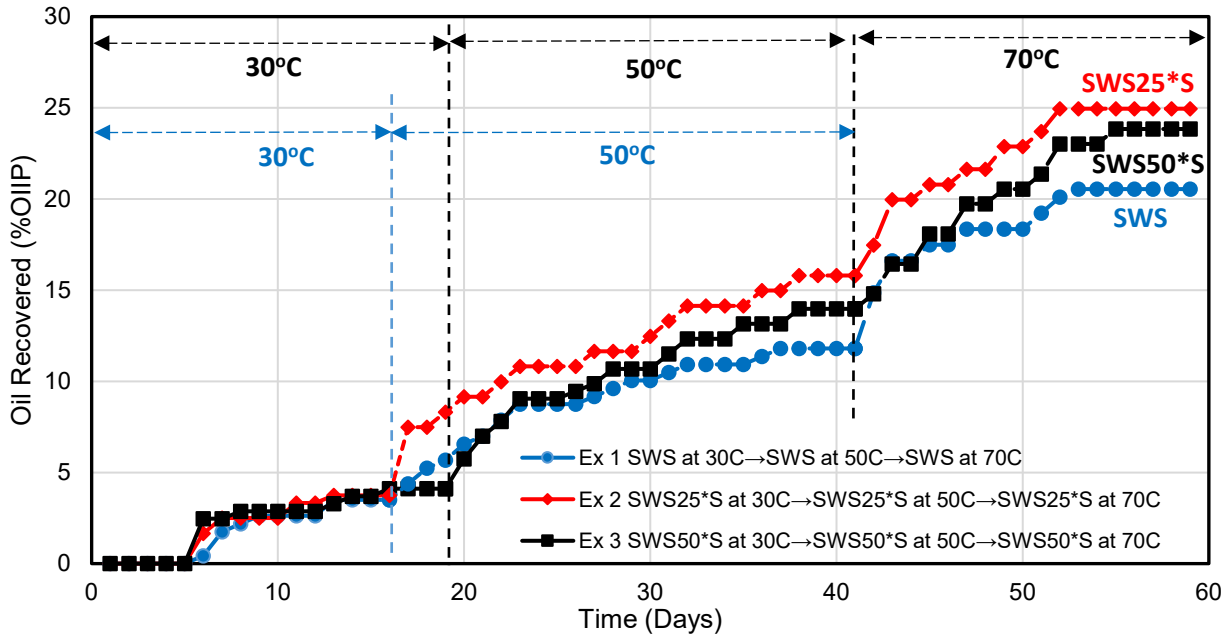

Figure 10: Oil recovery profile for Ex 1-3 during spontaneous imbibition at different temperatures. The effluent sample pH measured at the final imbibition at 70°C were 6.46, 6.52 and 6.62 for SWS, SWS25*S and SWS50*S respectively.

To fully explore the sulfate effect, bond product calculations were performed for Ex 1 to 3 at effluent pH. The BPS decreased slightly with increased sulfate concentration, indicating more water wetness and hence a better oil recovery (**Figure 11**A). As adsorption of SO_4^{2-} increased (**Figure 11**B), the concentration of the dominant electrostatic bond associated with carboxylic and amine groups, $[COO^-][CaOH_2^+]$ and $[NH^+][CO_3^-]$ respectively, decreased significantly. It should be noted that the number of $[COO^-][CaOH_2^+]$

bonds is marginally greater than the other associated bond linkages, hence its reduction would have a significant impact on the overall electrostatic attraction and play a major role in controlling wettability. Overall, the spontaneous imbibition results and the literature data are consistent with the BPS results. Lastly, increased temperature reduced the number of electrostatic bond linkages **(Figure 7 and 8),** increasing desorption of oil from calcite leading to more water wetness, consistent with experimental observations.

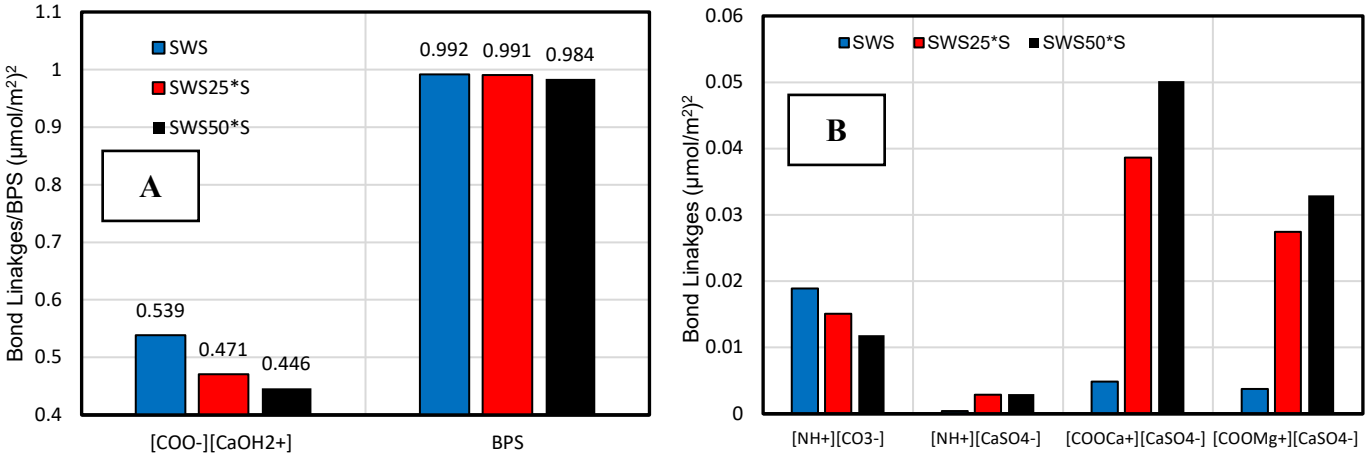

Figure 11: Contribution of electrostatic bond linkages to wettability alteration and improved oil recovery. A) shows the BPS and contribution of the dominant bond linkage ([COO-][$CaOH_2^+$]), B) shows electrostatic bond linkages associated with SO_4^{2-} adsorption.

Figure 12 shows spontaneous imbibition results from using SWS brine as the primary imbibing fluid. For secondary imbibition at 50°C, sulfate was kept constant for Ex 1 (SWS brine used) and increased 25 and 50 times for Ex 4 and 5 (SWS25*S and SWS50*S brine used, respectively). The temperature was raised to 70°C, with no further addition of sulfate, to isolate the interplay between sulfate and temperature. Total additional oil recovery at elevated temperature from both secondary and tertiary imbibition were observed to be 19.55%, 18.35% and 17.04% for SWS50*S, SWS25*S and SWS brines, respectively. Therefore, it could be concluded that, increased temperature increased oil recovery in the order: SWS<SWS25*S< SWS50*S (**Figure 12**). As observed in **Figure 7**, increasing the system temperature decreased the concentration of [>$CaOH_2^+$][-COO^-], [>CO_3^-][-NH^+] and [>$CaSO_4^-$][-NH^+] bonds from pH 5 to 7, i.e. the pH range of the imbibition experiments. Therefore, it would be expected that increased temperature would decrease the number of most abundant electrostatic bonds and alter rock wettability to improve oil recovery, as observed in **Figure 12**.

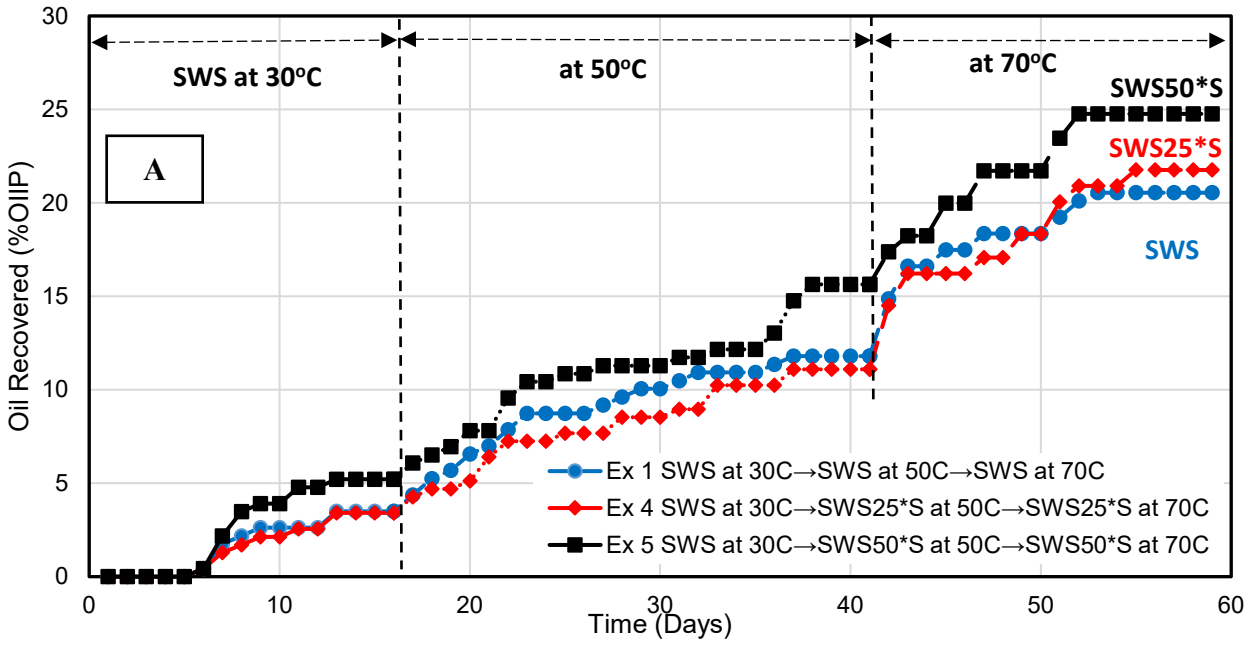

Figure 12: Oil recovery profile for Ex1, 4 and 5 during spontaneous imbibition at different temperature. For all the experiments, SWS brine was used as the primary imbibition fluid to serve as a baseline.

3.6 Discussion

In general, **Figure 8** showed that, as the temperature increased for each brine, the BPS reduced, indicating an increase in water-wetness on the calcite surface. Also, low pH was favorable for water-wetness on a calcite interface indicated through a lower calculated BPS. BPS was also observed to be lower as sulfate ion concentrations increased in the brine solutions. These were all consistent with the literature. In a work by Xie et al [46], an increase in pH was observed to make the calcite surface more oil-wet. Brine pH of 3 and 8 were considered in their contact angle measurements. This observation was combined with contact angle analysis from other publications with similar trends [44], further confirming that lower pH is required to achieve a low water contact angle and hence a water-wet state. The use of BPS was adequate in predicting the wettability trends with respect to pH in their work. Therefore, the observation of increased water wetness as the pH decreases at temperatures above 50°C is consistent with literature.

The second general observation with the BPS (**Figure 8**) was that, water wetness generally increased with increasing temperatures for all brines used. Increasing temperature resulted in increase in oil recovered using different seawater-like brines during the imbibition process (**Figure 10** and **Figure 12**). Using spontaneous imbibition experiments, Zhang et al.,[12,79,85] observed that, increasing the temperature resulted in increasing the produced oil from the chalk for seawater-like brines. This resulted in outlining a temperature dependent recovery mechanism for waterflooding using seawater-like brines. Mahani et al [18], observed through contact angle measurements that increasing the system temperature resulted in a greater

wetter ability alteration. In maintaining the system temperature at 25°C and switching the brine solution from formation water (239,394 mg/L) to seawater brine (43,731 mg/L), water contact angle on limestone surface was observed to change marginally (2° units). However, limestone water contact angle was observed to shift lower by 15° units after switching brine solution from formation water to seawater brine using system temperature of 100°C. Lu et al [19], using a pure calcite substrate, observed consistently that increasing the temperature from 25°C to 65°C resulted in a reduction in the WCA using NaCl and MgCl brines with different concentration. These results support our assertion with the effect of temperature on carbonate wettability. From the BPS analysis, increased temperature triggered a reduced strength of the electrostatic bond linkages, hence desorption of oil molecules from the calcite surface leading to more water wetness. Importantly, this work shows that system temperature about above 50°C is required to trigger electrostatic desorption resulting in altering carbonate wettability.

The third observation from the BPS is that, increasing the SO_4^{2-} concentration resulted in reducing the BPS and hence increase water-wetness (**Figure 8**). Also, SO_4^{2-} concentration resulted in increasing the oil produced from limestone rock during spontaneous imbibition (**Figure 10** and **Figure 12**). Interestingly, 1,300 ppm of SO_4^{2-} concentration (SWS25*S) was observed to improved oil recovery the most when used for secondary imbibition. This indicated that an optimum SO_4^{2-} concentration could trigger oil recovery, minimizing the potential of scale formation. Dehaghani and Badizad [81] observed through contact angle measurements on limestones that, increasing the SO_4^{2-} concentration resulted in altering the limestone wettability back to water wetness. Purswani and Karpyn [78] and Alshakhs and Kovscek [30] both observed that, the presence of sulfate and magnesium ions improved the water wetness on carbonates through contact angle measurements. Fathi et al [13] and Zhang et al[12], observed through spontaneous imbibition test that spiking the seawater brine with sulfate ions resulted in an improved oil recovery from chalk cores, indicating an alteration in wettability to water wetness. All these observations in literature supports the analysis observed with the BPS and in the oil production experiments, that is, an increase in sulfate concertation increases the water wetness on calcite surface by reducing the electrostatic bond linkages, particular associated with both [>CaOH2+][-COO-] and [>CO3-][-NH+] bonds, which improves oil recovery.

In general, more data of zeta potential measurement at high temperature is required to fully understand the electrokinetic at the calcite-oil interface. Detailing the experimental condition used in the measurement would reduce the disparities between measured and predicted data, leading to understanding of the electrostatic controls at the calcite and oil surfaces. Techniques such as the streaming potential could be employed more to acquire such data for model fitting. Nevertheless, SCM could be a very useful tool incorporated into reservoir model to capture the electrostatic and geochemical interactions in the rock porous

media that influence the wettability state and oil recovery process.

4 Conclusion

An SCM predicted improved oil recovery data from spontaneous imbibition measurements by quantifying the electrostatic interactions at calcite and oil surfaces. SO_4^{2-} adsorbed to calcite surface reduced the magnitude of the calculated zeta potential by interacting with the $>CaOH_2^+$ surface species; the effect increased with increasing sulfate levels. SO_4^{2-} probably has little effect on the oil surface**.** An increase in sulfate reduced electrostatic bonding, particularly $[-COO^-][>CaOH_2^+]$ and $[-NH^+][>CO_3^-]$ bonds, resulting increased water wetness and better oil recovery.

Increasing temperature increased the calculated magnitude of the zeta potential at the oil surface from pH 5 to 8 by reducing the concentration of $-NH^+$ groups. Temperature decreases the concentration of $>CO_3^-$ on calcite surface at pH 5 - 7, but increases it at pH 8, shifting the calcite zeta potential accordingly. Thus, increasing temperature weakens the amine-carbonate electrostatic bonds ($[>CO_3^-][-NH^+]$), improving water-wetness. BPS calculations predict that increased temperature, increased sulfate and low pH favored water wetness of calcite.

Acknowledgements

Acknowledgment is made to the donors of the American Chemical Society Petroleum Research Fund (award number 59031-ND9) for support of this research. Sandia National Laboratories is a multimission laboratory managed and operated by National Technology and Engineering Solutions of Sandia, LLC, a wholly owned subsidiary of Honeywell International, Inc., for the U.S. Department of Energy's National Nuclear Security Administration under contract DE-NA-0003525. This paper describes objective technical results and analysis. Any subjective views or opinions that might be expressed in the paper do not necessarily represent the views of the U.S. Department of Energy or the United States Government.

Reference

[1] G.Q. Tang, N.R. Morrow, Salinity, Temperature, Oil Composition, and Oil Recovery by Waterflooding, SPE Reserv. Eng. 12 (1997) 269–276. https://doi.org/10.2118/36680-PA.

[2] T. Austad, Water-Based EOR in Carbonates and Sandstones-Chapter 13:New Chemical Understanding of the EOR Potential Using "Smart Water," Enhanc. Oil Recover. F. Case Stud. (2013) 301–335.

[3] E. Al Shalabi, K. Sepehnoori, Low Salinity and Engineered Water Injection for Sandstone and Carbonate Reservoirs, 2017.

[4] A.A. Yousef, S.H. Al-Saleh, A. Al-Kaabi, M.S. Al-Jawfi, Laboratory Investigation of the Impact of Injection-Water Salinity and Ionic Content on Oil Recovery From Carbonate Reservoirs, SPE

Reserv. Eval. Eng. 14 (2011) 578–593. https://doi.org/10.2118/137634-PA.
[5] A. a Yousef, J.S. Liu, G.W. Blanchard, S. Al-Saleh, T. Al-Zahrani, R.M. Al-Zahrani, H.I. Al-Tammar, N. Al-Mulhim, Smart Waterflooding: Industry, in: SPE Annu. Tech. Conf. Exhib., Society of Petroleum Engineers, 2012: pp. 8–10. https://doi.org/10.2118/159526-MS.
[6] D.A. Afekare, M. Radonjic, From Mineral Surfaces and Coreflood Experiments to Reservoir Implementations: Comprehensive Review of Low-Salinity Water Flooding (LSWF), Energy & Fuels. 31 (2017) 13043–13062. https://doi.org/10.1021/acs.energyfuels.7b02730.
[7] A.N. Awolayo, H.K. Sarma, L.X. Nghiem, Brine-dependent recovery processes in carbonate and sandstone petroleum reservoirs: Review of laboratory-field studies, interfacial mechanisms and modeling attempts, Energies. 11 (2018). https://doi.org/10.3390/en11113020.
[8] J.T. Tetteh, P. V. Brady, R.B. Ghahfarokhi, Review of low salinity waterflooding in carbonate rocks: mechanisms, investigation techniques, and future directions, Adv. Colloid Interface Sci. (2020) 102253. https://doi.org/10.1016/j.cis.2020.102253.
[9] M. Seyyedi, S. Tagliaferri, J. Abatzis, S.M. Nielsen, An integrated experimental approach to quantify the oil recovery potential of seawater and low-salinity seawater injection in North Sea chalk oil reservoirs, Fuel. 232 (2018) 267–278. https://doi.org/10.1016/j.fuel.2018.05.158.
[10] R.A. Nasralla, E. Sergienko, S.K. Masalmeh, H.A. van der Linde, N.J. Brussee, H. Mahani, B.M.J.M. Suijkerbuijk, I.S.M. Al-Qarshubi, Potential of Low-Salinity Waterflood To Improve Oil Recovery in Carbonates: Demonstrating the Effect by Qualitative Coreflood, SPE J. 21 (2016) 1643–1654. https://doi.org/10.2118/172010-PA.
[11] R.A. Nasralla, H. Mahani, H.A. van der Linde, F.H.M. Marcelis, S.K. Masalmeh, E. Sergienko, N.J. Brussee, S.G.J. Pieterse, S. Basu, Low salinity waterflooding for a carbonate reservoir: Experimental evaluation and numerical interpretation, J. Pet. Sci. Eng. 164 (2018) 640–654. https://doi.org/10.1016/j.petrol.2018.01.028.
[12] P. Zhang, M.T. Tweheyo, T. Austad, Wettability alteration and improved oil recovery by spontaneous imbibition of seawater into chalk : Impact of the potential determining ions Ca 2 + , Mg 2 + , and SO 42 −, 301 (2007) 199–208. https://doi.org/10.1016/j.colsurfa.2006.12.058.
[13] S.J. Fathi, T. Austad, S. Strand, Water-based enhanced oil recovery (EOR) by “smart water”: Optimal ionic composition for EOR in carbonates, Energy and Fuels. 25 (2011) 5173–5179. https://doi.org/10.1021/ef201019k.
[14] P. Zhang, M.T. Tweheyo, T. Austad, Wettability alteration and improved oil recovery in chalk: The effect of calcium in the presence of sulfate, Energy and Fuels. 20 (2006) 2056–2062. https://doi.org/10.1021/ef0600816.
[15] T. Austad, S.F. Shariatpanahi, S. Strand, H. Aksulu, T. Puntervold, Low Salinity EOR Effects in Limestone Reservoir Cores Containing Anhydrite: A Discussion of the Chemical Mechanism, Energy and Fuels. 29 (2015) 6903–6911. https://doi.org/10.1021/acs.energyfuels.5b01099.
[16] M.A. Sohal, S. Kucheryavskiy, G. Thyne, E.G. Søgaard, Study of Ionically Modified Water Performance in the Carbonate Reservoir System by Multivariate Data Analysis, Energy & Fuels. 31 (2017) 2414–2429. https://doi.org/10.1021/acs.energyfuels.6b02292.
[17] J. Song, Q. Wang, I. Shaik, M. Puerto, P. Bikkina, C. Aichele, S.L. Biswal, G.J. Hirasaki, Effect of salinity, Mg2+ and SO42− on “smart water”-induced carbonate wettability alteration in a model oil system, J. Colloid Interface Sci. 563 (2020) 145–155. https://doi.org/10.1016/j.jcis.2019.12.040.
[18] H. Mahani, R. Menezes, S. Berg, A. Fadili, R. Nasralla, D. Voskov, V. Joekar-Niasar, Insights into the Impact of Temperature on the Wettability Alteration by Low Salinity in Carbonate Rocks, Energy and Fuels. 31 (2017) 7839–7853. https://doi.org/10.1021/acs.energyfuels.7b00776.
[19] Y. Lu, N.F. Najafabadi, A. Firoozabadi, Effect of Temperature on Wettability of Oil/Brine/Rock Systems, Energy and Fuels. 31 (2017) 4989–4995. https://doi.org/10.1021/acs.energyfuels.7b00370.

[20] S. Strand, S.C. Henningsen, T. Puntervold, T. Austad, Favorable Temperature Gradient for Maximum Low-Salinity Enhanced Oil Recovery Effects in Carbonates, Energy & Fuels. 31 (2017) 4687–4693. https://doi.org/10.1021/acs.energyfuels.6b03019.
[21] J.T. Tetteh, S. Alimoradi, P. V. Brady, R. Barati Ghahfarokhi, Electrokinetics at calcite-rich limestone surface: Understanding the role of ions in modified salinity waterflooding, J. Mol. Liq. 297 (2020) 111868. https://doi.org/10.1016/j.molliq.2019.111868.
[22] J.T. Tetteh, M. Veisi, P. V. Brady, R. Barati Ghahfarokhi, Surface Reactivity Analysis of the Crude Oil–Brine–Limestone Interface for a Comprehensive Understanding of the Low-Salinity Waterflooding Mechanism, Energy & Fuels. (2020) acs.energyfuels.9b03664. https://doi.org/10.1021/acs.energyfuels.9b03664.
[23] H. Mahani, A.L. Keya, S. Berg, W.B. Bartels, R. Nasralla, W.R. Rossen, Insights into the mechanism of wettability alteration by low-salinity flooding (LSF) in carbonates, Energy and Fuels. 29 (2015). https://doi.org/10.1021/ef5023847.
[24] M.D. Jackson, D. Al-Mahrouqi, J. Vinogradov, Zeta potential in oil-water-carbonate systems and its impact on oil recovery during controlled salinity water-flooding, Sci. Rep. 6 (2016) 37363. https://doi.org/10.1038/srep37363.
[25] A. Alroudhan, J. Vinogradov, M.D. Jackson, Zeta potential of intact natural limestone: Impact of potential-determining ions Ca, Mg and SO4, Colloids Surfaces A Physicochem. Eng. Asp. 493 (2016) 83–98. https://doi.org/10.1016/j.colsurfa.2015.11.068.
[26] S.R. Gomari, F. Amrouche, R.G. Santos, H.C. Greenwell, P. Cubillas, A new framework to quantify thewetting behaviour of carbonate rock surfaces based on the relationship between zeta potential and contact angle, Energies. 13 (2020). https://doi.org/10.3390/en13040993.
[27] H. Guo, N. Nazari, S. Esmaeilzadeh, A.R. Kovscek, A Critical Review of the Role of Thin Liquid Films for Modified Salinity Brine Recovery Processes, Curr. Opin. Colloid Interface Sci. 50 (2020) 101393. https://doi.org/10.1016/j.cocis.2020.101393.
[28] H. Ding, S. Rahman, Experimental and theoretical study of wettability alteration during low salinity water flooding-an state of the art review, Colloids Surfaces A Physicochem. Eng. Asp. 520 (2017) 622–639. https://doi.org/10.1016/j.colsurfa.2017.02.006.
[29] G.J. Hirasaki, Wettability: Fundamentals and Surface Forces, SPE Form. Eval. 6 (1991) 217–226. https://doi.org/10.2118/17367-PA.
[30] M.J. Alshakhs, A.R. Kovscek, Understanding the role of brine ionic composition on oil recovery by assessment of wettability from colloidal forces, Adv. Colloid Interface Sci. 233 (2016) 126–138. https://doi.org/10.1016/j.cis.2015.08.004.
[31] J. Tetteh, N.M. Janjang, R. Barati, Wettability alteration and enhanced oil recovery using low salinity waterflooding in limestone rocks: A mechanistic study, in: Soc. Pet. Eng. - SPE Kingdom Saudi Arab. Annu. Tech. Symp. Exhib. 2018, SATS 2018, 2018.
[32] A. Sari, Q. Xie, Y. Chen, A. Saeedi, E. Pooryousefy, Drivers of Low Salinity Effect in Carbonate Reservoirs, Energy and Fuels. 31 (2017) 8951–8958. https://doi.org/10.1021/acs.energyfuels.7b00966.
[33] A. Gandomkar, M.R. Rahimpour, The impact of monovalent and divalent ions on wettability alteration in oil/low salinity brine/limestone systems, J. Mol. Liq. 248 (2017) 1003–1013. https://doi.org/10.1016/j.molliq.2017.10.095.
[34] Y. Lu, N.F. Najafabadi, A. Firoozabadi, Effect of Temperature on Wettability of Oil/Brine/Rock Systems, Energy & Fuels. 31 (2017) 4989–4995. https://doi.org/10.1021/acs.energyfuels.7b00370.
[35] H. Collini, S. Li, M.D. Jackson, N. Agenet, B. Rashid, J. Couves, Zeta potential in intact carbonates at reservoir conditions and its impact on oil recovery during controlled salinity waterflooding, Fuel. 266 (2020) 116927. https://doi.org/10.1016/j.fuel.2019.116927.
[36] S.C. Ayirala, S.H. Saleh, S.M. Enezi, A.A. Al-yousef, S. Aramco, Effect of Salinity and Water Ions

on Electrokinetic Interactions in Carbonate Reservoir Cores at Elevated Temperatures, SPE J. (2018) 1–14.
[37] H. Mahani, A.L. Keya, S. Berg, R. Nasralla, Electrokinetics of Carbonate/Brine Interface in Low-Salinity Waterflooding: Effect of Brine Salinity, Composition, Rock Type, and pH on zeta-potential and a Surface-Complexation Model, SPE J. 22 (2017) 053–068. https://doi.org/10.2118/181745-PA.
[38] S. Erzuah, I. Fjelde, A.V. Omekeh, Wettability Estimation Using Surface-Complexation Simulations, SPE Reserv. Eval. Eng. 22 (2019) 509–519. https://doi.org/10.2118/185767-PA.
[39] M. Takeya, A. Ubaidah, M. Shimokawara, H. Okano, T. Nawa, Y. Elakneswaran, Crude oil/brine/rock interface in low salinity waterflooding: Experiments, triple-layer surface complexation model, and DLVO theory, J. Pet. Sci. Eng. 188 (2020) 106913. https://doi.org/10.1016/j.petrol.2020.106913.
[40] M. Bonto, A.A. Eftekhari, H. M. Nick, Wettability Indicator Parameter Based on the Thermodynamic Modeling of Chalk-Oil-Brine Systems, Energy & Fuels. 34 (2020) 8018–8036. https://doi.org/10.1021/acs.energyfuels.0c00716.
[41] A. Sari, Y. Chen, Q. Xie, A. Saeedi, Low salinity water flooding in high acidic oil reservoirs: Impact of pH on wettability of carbonate reservoirs, J. Mol. Liq. 281 (2019) 444–450. https://doi.org/10.1016/j.molliq.2019.02.081.
[42] P. V. Brady, G. Thyne, Functional Wettability in Carbonate Reservoirs, Energy and Fuels. 30 (2016) 9217–9225. https://doi.org/10.1021/acs.energyfuels.6b01895.
[43] P.V. Brady, J.L. Krumhansl, P.E. Mariner, Surface Complexation Modeling for Improved Oil Recovery, in: SPE Improv. Oil Recover. Symp., Society of Petroleum Engineers, 2012: pp. 14–18. https://doi.org/10.2118/153744-MS.
[44] Y. Chen, Q. Xie, A. Sari, P. V. Brady, A. Saeedi, Oil/water/rock wettability: Influencing factors and implications for low salinity water flooding in carbonate reservoirs, Fuel. 215 (2018) 171–177. https://doi.org/10.1016/j.fuel.2017.10.031.
[45] Y. Chen, A. Sari, Q. Xie, P. V. Brady, M.M. Hossain, A. Saeedi, Electrostatic Origins of CO2-Increased Hydrophilicity in Carbonate Reservoirs, Sci. Rep. 8 (2018) 17691. https://doi.org/10.1038/s41598-018-35878-3.
[46] Q. Xie, A. Sari, W. Pu, Y. Chen, P. V. Brady, N. Al Maskari, A. Saeedi, pH effect on wettability of oil/brine/carbonate system: Implications for low salinity water flooding, J. Pet. Sci. Eng. 168 (2018) 419–425. https://doi.org/10.1016/j.petrol.2018.05.015.
[47] M. Takeya, M. Shimokawara, Y. Elakneswaran, T. Nawa, S. Takahashi, Predicting the electrokinetic properties of the crude oil/brine interface for enhanced oil recovery in low salinity water flooding, Fuel. 235 (2019) 822–831. https://doi.org/10.1016/j.fuel.2018.08.079.
[48] P. V. Brady, J.L. Krumhansl, A surface complexation model of oil–brine–sandstone interfaces at 100°C: Low salinity waterflooding, J. Pet. Sci. Eng. 81 (2012) 171–176. https://doi.org/10.1016/j.petrol.2011.12.020.
[49] Q. Xie, P. V. Brady, E. Pooryousefy, D. Zhou, Y. Liu, A. Saeedi, The low salinity effect at high temperatures, Fuel. 200 (2017) 419–426. https://doi.org/10.1016/j.fuel.2017.03.088.
[50] M. Mansi, M. Mehana, M. Fahes, H. Viswanathan, Thermodynamic modeling of the temperature impact on low-salinity waterflooding performance in sandstones, Colloids Surfaces A Physicochem. Eng. Asp. 586 (2020) 124207. https://doi.org/10.1016/j.colsurfa.2019.124207.
[51] A. Sanaei, S. Tavassoli, K. Sepehrnoori, Investigation of modified Water chemistry for improved oil recovery: Application of DLVO theory and surface complexation model, Colloids Surfaces A Physicochem. Eng. Asp. 574 (2019) 131–145. https://doi.org/10.1016/j.colsurfa.2019.04.075.
[52] K.K. Mohanty, S. Chandrasekhar, Wettability Alteration with Brine Composition in High Temperature Carbonate Reservoirs, in: SPE Annu. Tech. Conf. Exhib., Society of Petroleum

Engineers, 2013. https://doi.org/10.2118/166280-MS.
[53] J. Tetteh, N.M. Janjang, R. Barati, Wettability Alteration and Enhanced Oil Recovery Using Low Salinity Waterflooding in Limestone Rocks: A Mechanistic Study, in: SPE Kingdom Saudi Arab. Annu. Tech. Symp. Exhib., Society of Petroleum Engineers, 2018. https://doi.org/10.2118/192425-MS.
[54] J.T. Tetteh, R. Barati, Crude-Oil/Brine Interaction as a Recovery Mechanism for Low-Salinity Waterflooding of Carbonate Reservoirs, SPE Reserv. Eval. Eng. 22 (2019) 0877–0896. https://doi.org/10.2118/194006-PA.
[55] J.T. Tetteh, S.E. Cudjoe, S.A. Aryana, R. Barati Ghahfarokhi, Investigation into fluid-fluid interaction phenomenon during low salinity waterflooding using a reservoir-on-a-chip microfluidics model, J. Pet. Sci. Eng. (2020).
[56] D.L. Parkhurst, C.A.J. Appelo, PHREEQC (Version 3)-A Computer Program for Speciation, Batch-Reaction, One-Dimensional Transport, and Inverse Geochemical Calculations, 2013. https://doi.org/Rep. 99-4259.
[57] F. Heberling, P. Eng, J. Lützenkirchen, T.P. Trainor, D. Bosbach, M.A. Denecke, Structure and reactivity of the calcite–water interface, J. Colloid Interface Sci. 354 (2010) 843–857. https://doi.org/10.1016/j.jcis.2010.10.047.
[58] Y. Chen, A. Ubaidah, Y. Elakneswaran, V.J. Niasar, Q. Xie, Detecting pH and Ca2+ increase during low salinity waterflooding in carbonate reservoirs: Implications for wettability alteration process, J. Mol. Liq. 317 (2020) 114003. https://doi.org/10.1016/j.molliq.2020.114003.
[59] C.A.J. Appelo, D. Postma, Geochemistry, Groundwater and Pollution, A.A. Balkema Publishers, 2005.
[60] J.N. Israelachvili, Intermolecular and Surface Forces, 2011. https://doi.org/10.1017/CBO9781107415324.004.
[61] E.W. Al Shalabi, Modeling the Effect of Injecting Low Salinity Water on Oil Recovery from Carbonate Reservoirs, University of Texas at Austin, 2014.
[62] J. Song, Y. Zeng, L. Wang, X. Duan, M. Puerto, W.G. Chapman, S.L. Biswal, G.J. Hirasaki, Surface complexation modeling of calcite zeta potential measurements in brines with mixed potential determining ions (Ca2+, CO32−, Mg2+, SO42−) for characterizing carbonate wettability, J. Colloid Interface Sci. 506 (2017) 169–179. https://doi.org/10.1016/j.jcis.2017.06.096.
[63] A. Sanaei, S. Tavassoli, K. Sepehrnoori, Investigation of modified Water chemistry for improved oil recovery: Application of DLVO theory and surface complexation model, Colloids Surfaces A Physicochem. Eng. Asp. 574 (2019) 131–145. https://doi.org/10.1016/j.colsurfa.2019.04.075.
[64] H. Ding, S.R. Rahman, Investigation of the Impact of Potential Determining Ions from Surface Complexation Modeling, Energy & Fuels. 32 (2018) 9314–9321. https://doi.org/10.1021/acs.energyfuels.8b02131.
[65] M. Wolthers, L. Charlet, P. Van Cappellen, The surface chemistry of divalent metal carbonate minerals: A critical assessment of surface charge and potential data using the charge distribution multi-site ion complexation model, Am. J. Sci. 308 (2008) 905–941. https://doi.org/10.2475/08.2008.02.
[66] W. Anderson, Wettability Literature Survey- Part 2: Wettability Measurement, J. Pet. Technol. 38 (1986) 1246–1262. https://doi.org/10.2118/13933-PA.
[67] L. Cuiec, Rock/Crude-Oil Interactions and Wettability: An Attempt To Understand Their Interrelation, in: SPE 59th Annu. Tech. Conf. Exhib. Houston, Texas, 1984.
[68] M.B. Alotaibi, A. Yousef, The Role of Individual and Combined Ions in Waterflooding Carbonate Reservoirs: Electrokinetic Study, SPE Reserv. Eval. Eng. 20 (2017) 77–86.
[69] J.T. Tetteh, Nano to Macro Scale Investigation into Low Salinity Waterflooding in Carbonate Rocks, in: SPE Annu. Tech. Conf. Exhib., Society of Petroleum Engineers, 2020.

https://doi.org/10.2118/204276-STU.
[70] M.B. Alotaibi, D. Cha, A.M. Alsofi, A.A. Yousef, Dynamic interactions of inorganic species at carbonate/brine interfaces: An electrokinetic study, Colloids Surfaces A Physicochem. Eng. Asp. 550 (2018) 222–235. https://doi.org/10.1016/j.colsurfa.2018.04.042.
[71] J.T. Tetteh, S. Alimoradi, P.V. Brady, R. Barati Ghahfarokhi, Electrokinetics at calcite-rich limestone surface: Understanding the role of ions in modified salinity waterflooding, J. Mol. Liq. 297 (2020). https://doi.org/10.1016/j.molliq.2019.111868.
[72] P. Zhang, T. Austad, Wettability and oil recovery from carbonates: Effects of temperature and potential determining ions, Colloids Surfaces A Physicochem. Eng. Asp. 279 (2006) 179–187. https://doi.org/10.1016/j.colsurfa.2006.01.009.
[73] P. V. Brady, N.R. Morrow, A. Fogden, V. Deniz, N. Loahardjo, A. Winoto, Electrostatics and the low salinity effect in sandstone reservoirs, Energy and Fuels. 29 (2015) 666–677. https://doi.org/10.1021/ef502474a.
[74] A. Saeedi, L. You, Y. Chen, Q. Xie, M. Hossain, Drivers of Wettability Alteration for Oil/Brine/Kaolinite System: Implications for Hydraulic Fracturing Fluids Uptake in Shale Rocks, Energies. 11 (2018) 1666. https://doi.org/10.3390/en11071666.
[75] P. V. Brady, J.L. Krumhansl, Surface Complexation Modeling for Waterflooding of Sandstones, SPE J. 18 (2013) 214–218. https://doi.org/10.2118/163053-pa.
[76] N.S. Al Maskari, A. Sari, M.M. Hossain, A. Saeedi, Q. Xie, Response of non-polar oil component on low salinity effect in carbonate reservoirs: Adhesion force measurement using atomic force microscopy, Energies. 13 (2019) 13–15. https://doi.org/10.3390/en13010077.
[77] S.J. Fathi, T. Austad, S. Strand, "smart water" as a wettability modifier in chalk: The effect of salinity and ionic composition, Energy and Fuels. 24 (2010) 2514–2519. https://doi.org/10.1021/ef901304m.
[78] P. Purswani, Z.T. Karpyn, Laboratory investigation of chemical mechanisms driving oil recovery from oil-wet carbonate rocks, Fuel. 235 (2019) 406–415. https://doi.org/10.1016/j.fuel.2018.07.078.
[79] P. Zhang, T. Austad, Wettability and oil recovery from carbonates: Effects of temperature and potential determining ions, Colloids Surfaces A Physicochem. Eng. Asp. 279 (2006) 179–187. https://doi.org/10.1016/j.colsurfa.2006.01.009.
[80] H. Ding, S. Mettu, S.S. Rahman, Impacts of Smart Waters on Calcite-Crude Oil Interactions Quantified by "soft Tip" Atomic Force Microscopy (AFM) and Surface Complexation Modeling (SCM), Ind. Eng. Chem. Res. (2020). https://doi.org/10.1021/acs.iecr.0c03643.
[81] A.H. Saeedi Dehaghani, M.H. Badizad, Impact of ionic composition on modulating wetting preference of calcite surface: Implication for chemically tuned water flooding, Colloids Surfaces A Physicochem. Eng. Asp. 568 (2019) 470–480. https://doi.org/10.1016/j.colsurfa.2019.02.009.
[82] H. Ding, S. Mettu, S. Rahman, Probing the Effects of Ca2+, Mg2+, and SO42-on Calcite-Oil Interactions by "soft Tip" Atomic Force Microscopy (AFM), Ind. Eng. Chem. Res. 59 (2020) 13069–13078. https://doi.org/10.1021/acs.iecr.0c01665.
[83] T. Austad, Water Based EOR in Carbonates and Sandstones : New Chemical Understanding of the EOR-Potential Using " Smart Water ," Enhanc. Oil Recover. F. Cases. (2013) 301–332.
[84] A. Awolayo, H. Sarma, A. AlSumaiti, An Experimental Investigation into the Impact of Sulfate Ions in Smart Water to Improve Oil Recovery in Carbonate Reservoirs, Transp. Porous Media. 111 (2016) 649–668. https://doi.org/10.1007/s11242-015-0616-4.
[85] B.M.J.M. Suijkerbuijk, H.P.C.E. Kuipers, C.P.J.W. Van Kruijsdijk, S. Berg, J.F. van Winden, D.J. Ligthelm, H. Mahani, M. Pingo Almada, E. van den Pol, V. Joekar Niasar, J. Romanuka, E.C.M. Vermolen, I.S.M. Al-Qarshubi, The Development of a Workflow to Improve Predictive Capability of Low Salinity Response, in: Int. Pet. Technol. Conf., International Petroleum Technology Conference, 2013. https://doi.org/10.2523/IPTC-17157-MS.

Impact of Temperature and SO_4^{2-} on Electrostatic Controls over Carbonate Wettability

Joel T. Tetteh[1*], Patrick V. Brady[2] and Reza Barati Ghahfarokhi[1]

[1] Department of Chemical and Petroleum Engineering, University of Kansas

[2] Sandia National Laboratories, USA

[*]Correspondence to: Joel T. Tetteh (E-mail: joel_tetteh@ku.edu)

Supporting Information.

This section provide supporting documents to the manuscript.

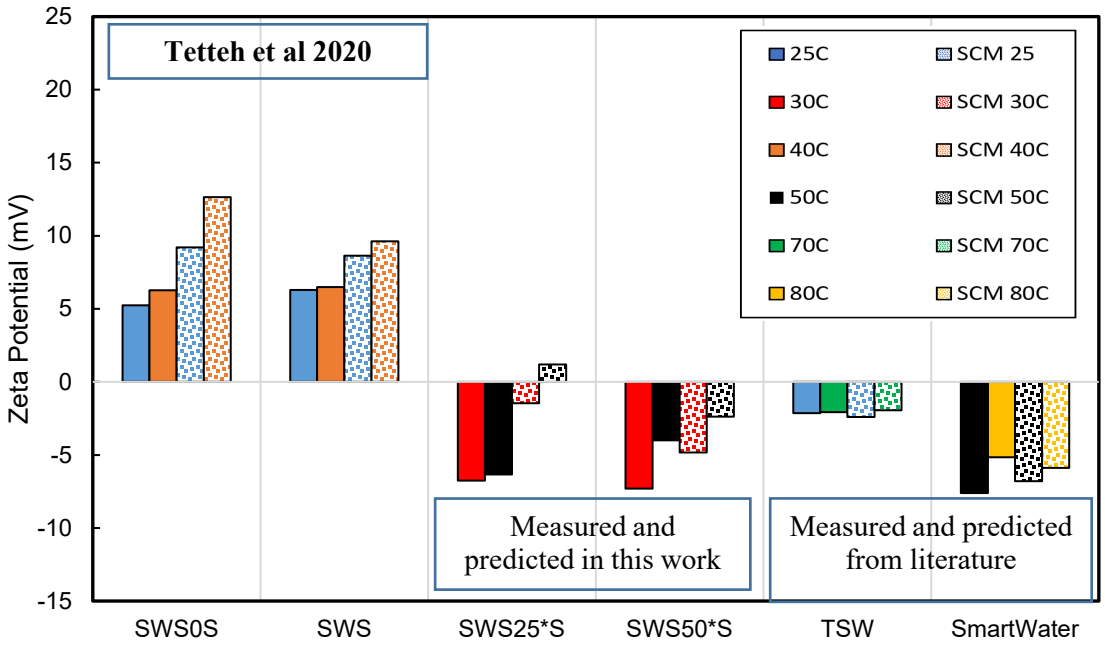

Figure A1: Model validation of predicted zeta potential of calcite surfaces using SCM against measured zeta potential by Tetteh et al (2020) at 25 and 40°C, Collini et al (2020) at 25°C (blue bar) and 70°C (green bar), and Alotaibi and Yousef, (2017) at 50°C (black bar) and 80°C (yellow bar).

1

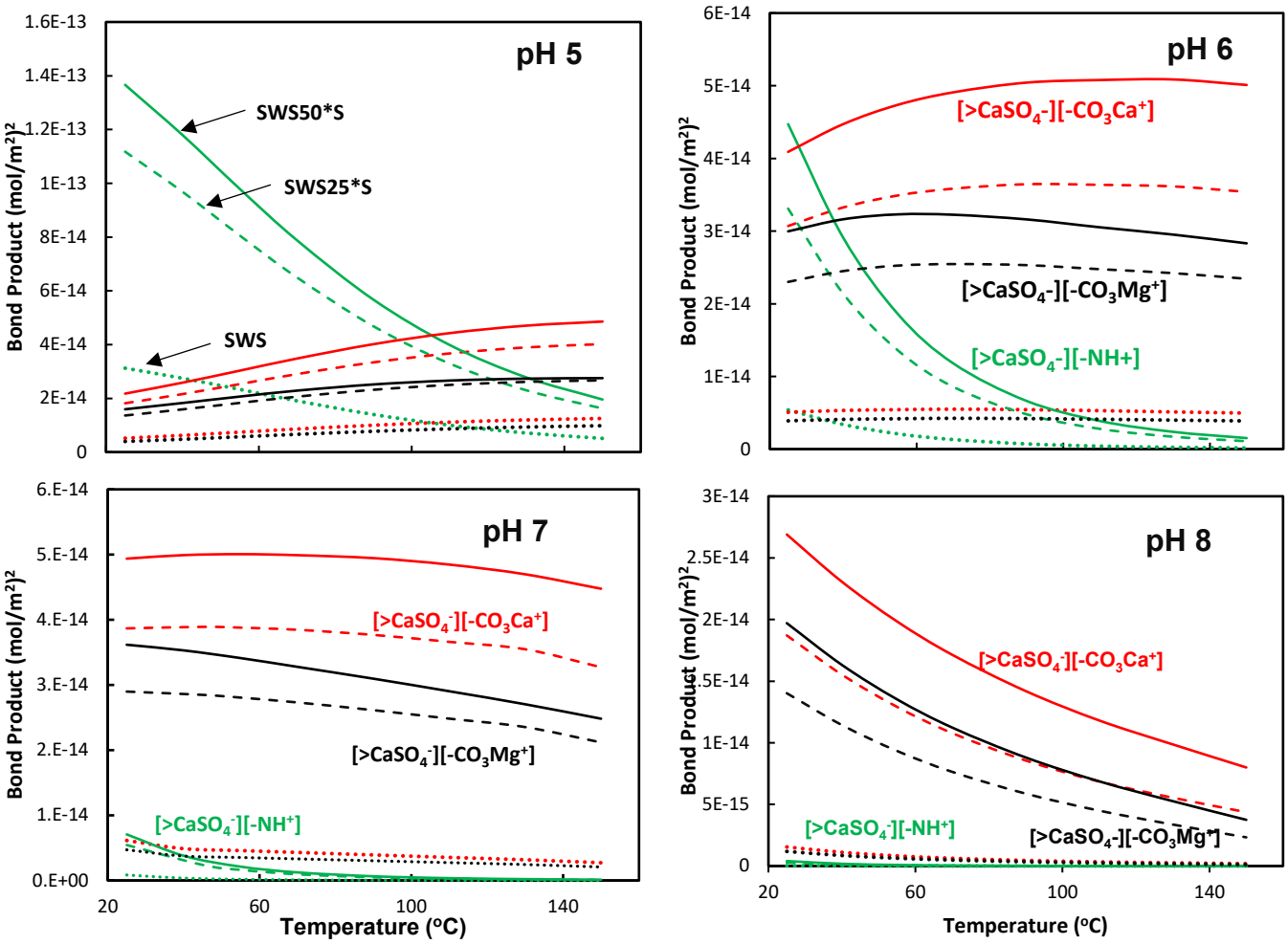

2
3 *Figure A2: Variation in electrostatic bond linkages associated with [>CaSO$_4^-$] species as a function of system temperature at pH 5 to 8.*
4
5